Available online at www.sciencedirect.com
SCIENCE DIRECT
ELSEVIER
Deep-Sea Research I 52 (2005) 1591–1615
DEEP-SEA RESEARCH
PART I
www.elsevier.com/locate/dsr

Changing sedimentary environment during the Late Quaternary: Sedimentological and isotopic evidence from the distal Bengal Fan

Pratima M. Kessarkar[a], V. Purnachandra Rao[a,*], S.M. Ahmad[b], S.K. Patil[c], A. Anil Kumar[a], G. Anil Babu[b], Sukalyan Chakraborty[a], R. Soundar Rajan[b]

[a]*National Institute of Oceanography, Dona Paula 403 004, Goa, India*
[b]*National Geophysical Research Institute, Hyderabad 500 007, India*
[c]*Indian Institute of Geo-magnetism, Alibagh 402 201, Maharashtra, India*

Received 20 April 2004; received in revised form 26 October 2004; accepted 27 January 2005
Available online 13 June 2005

Abstract

The sediments recovered from two gravity cores of the lower and distal Bengal Fan were investigated for sedimentological properties and Sr–Nd isotopes. Each core exhibits two distinct units, the lower unit 2 and upper unit 1 sediments. The unit 2 sediments are predominantly olive black/grey in colour with abundant finer silt-size fractions, low organic carbon and $CaCO_3$, quartz and mica in the coarse fraction, dominant illite and chlorite in the $<2\,\mu m$ fraction and uniform rock-magnetic properties. Biogenic constituents are extremely rare or restricted to the lower part of unit 2. The unit 1 sediments, on the other hand, are moderate brown/yellowish brown in colour with intermittent thin dark-coloured sediment layers. Higher clay, organic carbon, $CaCO_3$, and biogenic constituents in the coarse fraction, and enriched smectite and kaolinite in the $<2\,\mu m$ fraction are typical. Magnetic susceptibility values are higher and correlate well with acid-insoluble residue content. Higher Rb, Sr, Sm and Nd concentrations, $^{87}Sr/^{86}Sr$ ratios and more radiogenic ε_{Nd} values are characteristic for unit 2 sediments compared to unit 1 in both the cores. The unit 2 sediments represent Pleistocene hemiturbidites, older than 13 ^{14}C kyr BP with their source from the northern Bay of Bengal (NBOB), derived from the Himalayas and transported by the Ganges–Brahmaputra (G–B) River system. Unit 1 sediments are calcareous pelagic sediments, which started depositing ~12 ^{14}C kyr BP, with its clastic sediments derived from the Himalayas and SE Indian/Sri Lankan margins. The change in lithofacies from unit 2 to unit 1 suggests that the sediment deposition by turbidity current activity ceased in the distal Bengal Fan at ~12 ^{14}C kyr BP, perhaps because of the rapid rise in sea-level during the melt water pulse 1A and Holocene.

Keywords: Turbidites; Pelagic sediments; Provenance; Late Quaternary; Distal Bengal Fan

*Corresponding author. Fax: +91 832 2450609.
E-mail address: vprao@darya.nio.org (V.P. Rao).

0967-0637/$ - see front matter © 2005 Elsevier Ltd. All rights reserved.
doi:10.1016/j.dsr.2005.01.009

1. Introduction

The Modern Bengal Fan came into existence with the deposition of turbidite sediments since the Oligocene/Early Miocene (Cochran, 1990; Stow et al., 1990). Recent investigations on the deep-sea fan are directed largely to understand the (a) morphology and seismic stratigraphy of the submarine fan and growth and migration of submarine channels connecting the fan system,

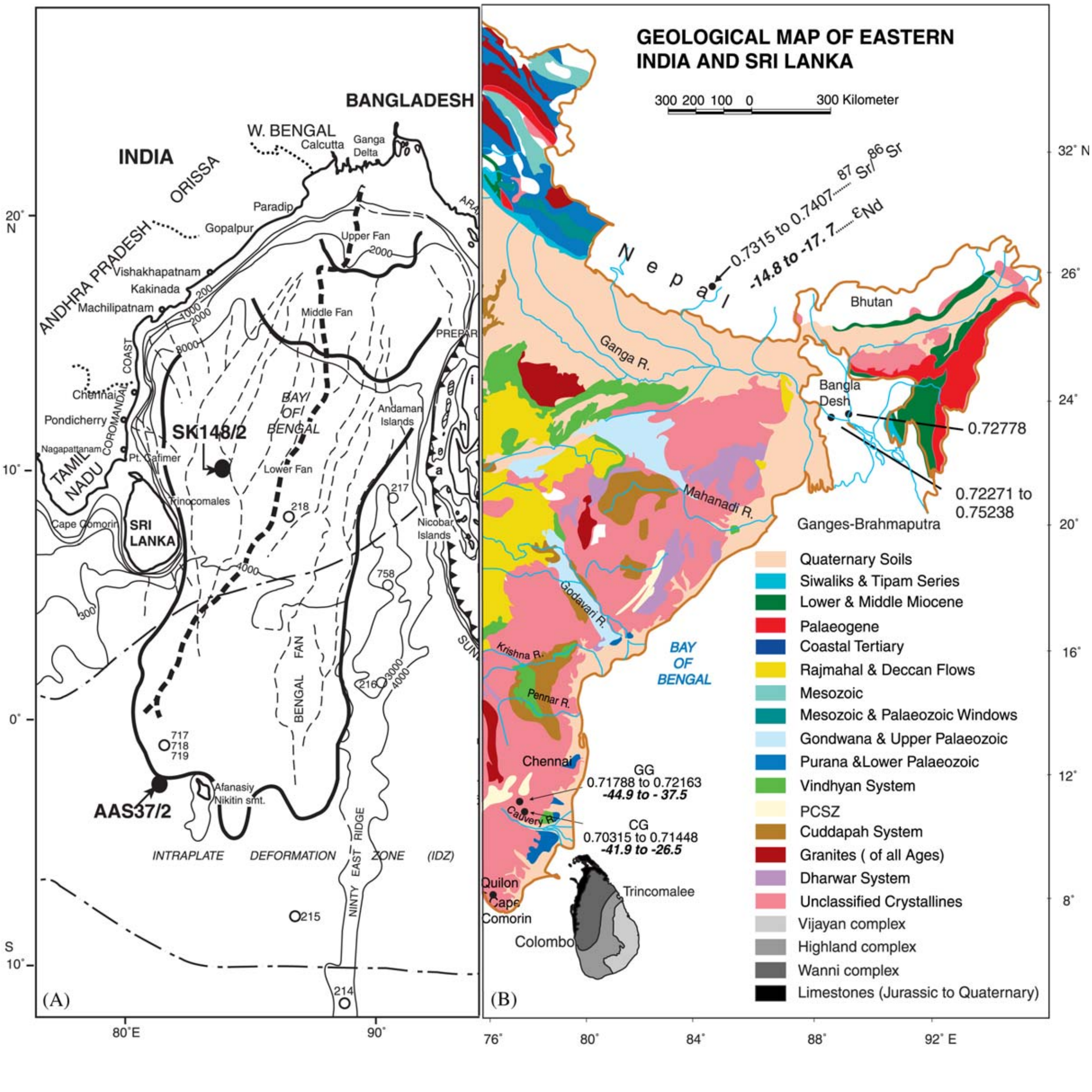

Fig. 1. (A) Locations of the sediment cores on the Bengal Fan. Boundaries of the Upper, Middle and Lower Fan regions, active turbidity current channel—thick dashed line, other turbidity channels—thin dashed lines, DSDP and ODP core sites are also shown (modified after Emmel and Curray, 1984). (B). Geology of Eastern India and Sri Lanka (Anonymous, 1965), Sr and Nd isotopes of the geological formations and Ganges river discharge are also given. GC-granitic gneiss and CG-charnokite gneiss (after Peucat et al., 1989; Galy et al., 1999; Dowling et al., 2003).

(b) controls on turbidite sedimentation and (c) composition and sources of the turbidites. Although the Bengal Fan is dissected by a number of modern and buried channels, recent investigations showed that, at present, only one channel exists connecting to the 'Swatch of No Ground' (Weber et al., 2003). Several canyons and channels also cut across the eastern Indian and Sri Lankan margins (Rao and Kessarkar, 2001) and supply sediments to the Western Fan (Fig. 1A). Several scholars showed no recent evidence of turbidite sediment accumulation in the lower Bengal Fan and suggested that the sediments are largely being trapped in the lower deltaic plain and shelf region (Curray and Moore, 1971; Curray et al., 1982; Emmel and Curray, 1985; Curray, 1994; Goodbread and Kuehl, 1999). Others, however, demonstrated the active growth of the fan during the most recent sea-level rise and high stand (Kuehl et al., 1989; Segall and Kuehl, 1992; Curray et al., 2003) with turbidites deposited right on the surface (Wetzel, 1990; Weber et al., 1997, 2003). Weber et al. (2003) further suggested that outside the active channel a large part of the fan is sediment starved and inactive during the Holocene sea-level high stand. Studies on other large deep sea fan systems such as the Amazon Fan, the Mississippi Fan and the Indus Fan also demonstrated that the changes in sea-level played a major role in turbidite sedimentation (Manley and Flood, 1988; Bouma et al., 1989; Kolla and Perlmutter, 1993; Prins et al., 2000). However, by using Sr concentrations and Sr–Nd isotopes it has been documented that tectonic activity in the Himalayas played a major role in sedimentation of turbidites in the Bengal Fan (Rea, 1992; France-Lanord et al., 1993). Further, it was demonstrated that the colour and mineralogy of the sediments might mislead one as to the sources of turbidites, but by using mineralogy together with radiogenic (Sr–Nd) and stable isotope (O–C) tracers a better understanding can be achieved regarding their provenance (Bouquillon et al., 1990; France-Lanord et al., 1993; Fagel et al., 1994; Derry and France-Lanord, 1996; Colin et al., 1999).

Here, we have investigated two sediment cores from the Bengal Fan (Fig. 1A; Table 1) for sedimentological properties, Sr–Nd concentrations and their isotopes. The purpose of this paper is to report the nature and sources of sediment supply and factors controlling their distribution in the lower and distal Bengal Fan during the Late Quaternary.

2. Previous studies

On the basis of different sedimentological parameters, types of turbidite facies in the Bengal Fan sediments were delineated from the DSDP and ODP core sites (von der Borch et al., 1972; Cochran et al., 1989; Stow et al., 1990). Clay mineral studies in the Bengal Fan are limited (Siddiquie, 1967; Goldberg and Griffin, 1970; Venkataratnam and Biscaye, 1973; Brass and Raman, 1990; Kolla and Rao, 1990; Suresh and Bagati, 1998; Colin et al., 1999; Chauhan and Suneethi, 2001). Clay minerals in the distal Bengal Fan are controlled by the relative rates of sediment supply from the Himalayan and Deccan sources. Illite and chlorite-rich sediments, derived from the Himalayas, are predominant in the Bengal Fan and can be traced to well south of the equator (Venkataratnam and Biscaye, 1973). Several workers reported smectite-rich sediments in the southwestern sector of the Bay of Bengal

Table 1
Details of sediment cores used in this study

Core no.	Research vessel	Cruise no/ core no.	Position (Lat. N, Long. E)	Water depth (m)	Length of the sediment core recovered (m)	Area (Bengal Fan)
Core 1 (SK148/2)	O.R.V. *Sagar Kanya*	148/2	10°00′00″, 84°00′00″	3600	3.46	Lower Western Fan
Core 2 (AAS37/2)	A.A. *Sidorenko*	37/2	02°25′12″, 81°02′36″	4000	1.14	Distal Fan

and kaolinite, illite and chlorite in the eastern sector (Siddiquie, 1967; Goldberg and Griffin, 1970; Venkataratnam and Biscaye, 1973). Some DSDP and ODP cores (Stow et al., 1990) and Shiva cores (Fagel et al., 1994, 1997) showed illite–chlorite (IC)-rich light grey sediments interlayered with smectite–kaolinite (SK)-rich dark grey sediments. Derry and France-Lanord (1996) subsequently demonstrated that the colour and mineralogy of the sediments might mislead as to the provenance and suggested that the turbidites rich in IC and SK clays were derived from the same source rocks but had undergone different alteration histories before reaching the Bengal Fan. Sediment traps also showed transport of clays from the Indian peninsula to the fan region (Ramaswamy et al., 1997).

The Sr–Nd isotopes of the turbidites revealed precise sources of Fan sediment (McLennan et al., 1990; Bouquillon et al., 1990; Derry and France-Lanord, 1996). It has been suggested that the source of the detrital sediment was essentially constant since the Early Miocene and dominantly Himalayan (Bouquillon et al., 1990; Derry and France-Lanord, 1996). Others proposed that a small part of the particulate budget is from the non-Himalayan component, such as the Indian or Sri Lankan sub-continents. For example, Fagel et al. (1994, 1997) reported major Himalayan sourced sediment with some contribution from the Chagos–Laccadive Ridge in the Central Indian Basin. Colin et al. (1999) suggested that the western part of the BOB sediments are essentially from the G–B River system, whereas the sediments in the eastern part are mixtures derived from the G–B River, the Irrawaddy River and the Arakan Coast. Pierson-Wickmann et al. (2001) showed geographic dependence of Sr–Nd distribution, which reflects the source variations by sediment transport processes and location in the Bay of Bengal. The Sr isotopic ratios of the carbonate fraction from the Bay of Bengal sediments (Rea 1992; Hohndorf et al., 2003) and Nd isotopes in the sediments of the eastern Indian Ocean and its relation to the genesis of island arc volcanism (Ben Othman et al., 1989) were also reported. The Sr–Nd of the particulate flux from the G–B Rivers (Sarin et al., 1989; Krishnaswamy et al., 1992; Galy et al., 1999; Galy and France-Lanord, 2001), different Deccan Traps formations (Lightfoot et al., 1990), southern Indian (Peucat et al., 1989) and Sri Lankan formations (Milisenda et al., 1994) were reported.

3. Geological setting and oceanographic conditions

The G–B River system, draining the Himalayas, is the largest sediment source, discharging enormous quantities of suspended and bed load (~1.06 billion tons/yr; Milliman and Syvitski, 1992) to the Bay of Bengal. It drains over Precambrian formations in the upper reaches and Rajmahal Traps and recent alluvium in the lower reaches under cold climatic conditions (Fig. 1B). The peninsular rivers are full only during and immediately after the SW monsoon (June to August) and bring largely the chemical weathering products. The Mahanadi, Brahmani, Vamsadhara and Nagavali drain over khondalites, granulites and charnockites of the Archean Eastern Ghat province (Fig. 1B). The Eastern Ghats are series of detached hills stretching intermittently from the northern border of Orissa through the coastal regions of the Andhra Pradesh and Tamil Nadu. Thick laterites and bauxites frequently cover the khondalites in the Eastern Ghats. The Godavari and Krishna Rivers rise through the Western Ghats, drain Deccan Traps in the upper reaches and pass through the Eastern Ghats and Quaternaries in the lower reaches (Krishnan, 1968). The Cauvery River also rises in the Western Ghats but drains through unclassified crystallines and Quaternaries (Fig. 1B).

The surface circulation in the Bay of Bengal is controlled by seasonal variations in winds (Shetye et al., 1993), where remotely forced coastally trapped waves and Rossby waves crossing the interior of the Bay are major contributors to the East Indian Coastal Current (EICC) variability (McCreary et al., 1996). During the summer (SW) monsoon the EICC bifurcates and flows northward north of 10°N and southwards off Sri Lanka (Eigenheer and Quadfasel, 2000). After the SW monsoon, pockets of coastal upwelling occur in certain regions, and a plume of low-salinity waters originating from the G–B River drift southward in the offshore region (Shetye et al., 1991). During the winter (NE) monsoon, the EICC begins to flow southwards along the east coast of India and Sri Lanka (Schott and McCreary, 2001) with a low salinity plume along the east coast (Shetye et al., 1996). The EICC also has southwestward flowing subsurface flow along the Indian coast that extends to depths greater than 1000 m from May to July and later forms into a coastal undercurrent (McCreary et al., 1996).

4. Material and methods

Two sediment gravity cores (core 1 and 2) collected during the 148th cruise of O.R.V. *Sagar Kanya* (SK148/2) and 37th cruise of A.A. *Siderenko* (AAS37/2) at water depths 3600 and 4000 m, respectively, from the western lower Bengal Fan and distal Bengal Fan (Fig. 1A; Table 1) were used for the present study. The sediments recovered are of 3.46 m length in core 1 and 1.14 m in core 2. Subsampling of sediment cores was done onboard at 2 cm intervals, and the colour of the sediment was noted. The $CaCO_3$ content was determined by rapid gasometric technique, following Hulsemann (1966). Reproducibility of the measurements, as checked by running replicates of samples, was found to be better than $\pm 5\%$. The acid-insoluble residue (AIR) was calculated by subtracting the carbonate percentage from the total. The organic carbon (OC) and total nitrogen (TN) were determined on a CNS elemental analyser (NCS 2500) (Tables 2A–B; Figs. 2A–B). The reproducibility of the OC measurements was found to be better than $\pm 1\%$. Coarse fraction constituents were observed under binocular microscope (Tables 2A–B). Bulk sediments (with and without carbonate) were also examined under a JEOL 5800 LV scanning electron microscope for biogenic constituents. Grain size measurements were carried out on the carbonate- and organic-matter-free mud fraction ($<63\,\mu m$ size), with a Malvern laser particle size analyzer (Master-Sizer 2000). Following Wentworth's classification (Folk, 1968) the mud fraction of the sediment was divided into different size grades (Figs. 3A–B).

The $<2\,\mu m$ fraction of the sediment was separated by settling velocity principle and oriented clay slides were prepared by pipetting 1 ml clay solution onto glass slides and allowing them to dry in air. The remaining clay sample ($<2\,\mu m$ fraction) was dried, powdered and used for Sr–Nd isotope measurements. The air-dried and ethylene glycol treated (at 100 °C for 1 h) clay slides were scanned from 2° to 22° 2θ at 1° 2θ/min on a Philips X-ray diffractometer using nickel-filtered Cu Kα radiation. Slow scan X-ray diffraction from 24° to 26° 2θ at 0.5° 2θ/min was also carried out for each slide. Clay minerals were identified and quantified (Tables 2A–B; Figs. 4A–B), following Biscaye (1965).

Magnetic susceptibility (MS) was determined on dried samples using a Bartington MS-2 magnetic susceptibility meter (with an AC magnetic field amplitude of 80 A/m) linked to a MS2B dual frequency sensor at the Indian Institute of Geomagnetism (IIG), Alibagh, India. Low frequency, χ_{lf}, (0.47 kHz) and high frequency χ_{hf}, (4.7 kHz) magnetic susceptibilities were measured on 0.1 range for three times on each sample and the averages of three measurements are presented as mass specific values in $10^{-8}\,m^3/kg$ SI units. Anhysteretic remanent magnetization (ARM) was imparted on the samples by superposing a DC biasing field of 0.05 mT on a smoothly decreasing alternating field with a peak of 100 mT. It is customary to express ARM as an anhysteretic susceptibility χ_{ARM} (mass specific ARM/strength of the biasing field). Isothermal remanent magnetization (IRM) acquisition was carried out using a Molspin pulse magnetizer and remanences were measured by Molspin spinner magnetometer. Saturation isothermal remanent magnetization (SIRM) was imparted using a maximum field of 1 T. After acquisition of SIRM, the samples were subjected to reverse DC fields of 0.3 T and the remanence was measured by using the Molspin magnetometer. The ratios of χ_{ARM}/SIRM and χ_{ARM}/χ_{lf}, S-ratio% and HIRM (hard IRM) were calculated by using the definitions of Robinson (1986) and Bloemendal et al. (1992) (see Figs. 5A–B).

The carbonate-free sediments (eight samples from each core) were treated with a mixture

Table 2A
Distribution of $CaCO_3$, OC, TN, coarse fraction constituents and clay minerals in SK 148/2

Depth (cm)	$CaCO_3$ (wt%)	OC (wt%)	TN (wt%)	OC/TN	Coarse fraction constituents				Clay minerals					
					B (%)	P (%)	K (%)	B/P	S (%)	I (%)	K (%)	Ch (%)	S/I	K/Ch
0	43	0.62	0.08	7.6	NA	NA	NA	NA	3.9	63.8	21.7	10.6	0.1	2.1
4	41	0.53	0.07	7.1	4	1	95	5.3	0	40.9	13.0	46.1	0	0.3
10	40	0.47	0.06	7.7	2	28	70	0.1	2.3	52.6	25.5	19.6	0.0	1.3
14	43	0.82	0.1	8.2	5	41	54	0.1	3.8	43.6	10.0	42.6	0.1	0.2
18	44	0.6	0.07	8.2	1	27	72	0	13.3	49.5	23.4	13.8	0.3	1.7
22	40	0.5	0.06	7.9	1	28	71	0	5.1	24.2	28.5	42.2	0.2	0.7
26	47	0.5	0.06	8.3	2	32	66	0.1	3.5	67.4	19.5	9.5	0.1	2.1
30	46	0.47	0.05	9.2	4	14	82	0.3	NA	NA	NA	NA	NA	NA
34	45	0.52	0.05	10.0	4	14	82	0.3	NA	NA	NA	NA	NA	NA
38	50	0.69	0.07	10.6	2	38	60	0	NA	NA	NA	NA	NA	NA
42	47	0.81	0.07	10.9	3	44	53	0.1	22.3	55.7	9.5	12.4	0.4	0.8
46	44	0.92	0.08	11.8	4	35	61	0.1	10.6	57.1	13.7	18.6	0.2	0.7
50	43	0.93	0.08	11.5	4	63	34	0.1	NA	NA	NA	NA	NA	NA
54	38	0.98	0.09	11.5	10	46	44	0.2	3.8	69.2	9.6	17.3	0.1	0.6
58	30	1.03	0.08	12.6	6	55	39	0.1	6.4	66.0	15.6	12.1	0.1	1.3
62	35	0.62	0.07	8.6	3	17	80	0.2	9.8	65.1	11.2	14.0	0.1	0.8
66	44	0.72	0.08	8.6	4	37	59	0.1	NA	NA	NA	NA	NA	NA
70	42	0.73	0.08	9.1	4	32	64	0.1	9.2	62.4	10.3	18.1	0.1	0.6
74	47	0.68	0.07	10.2	3	7	90	0.5	NA	NA	NA	NA	NA	NA
78	47	0.51	0.06	9.3	2	28	70	0.1	5.8	53.3	18.8	22.1	0.1	0.8
82	48	0.41	0.05	8.9	2	15	83	0.1	5.0	70.6	16.5	7.8	0.1	2.1
86	47	0.41	0.05	8.6	3	25	72	0.1	7.7	61.2	19.0	12.2	0.1	1.6
90	47	0.61	0.06	10.7	1	32	67	0	NA	NA	NA	NA	NA	NA
94	50	0.71	0.07	10.0	2	40	58	0.1	5.0	53.3	25.5	16.2	0.1	1.6
98	44	0.75	0.07	11.5	6	32	62	0.2	24.6	57.4	7.4	10.6	0.4	0.7
102	49	0.91	0.08	11.6	11	40	49	0.3	NA	NA	NA	NA	NA	NA
106	44	1.06	0.09	12.2	6	56	38	0.1	26.1	58.0	6.4	9.5	0.5	0.7
112	39	0.96	0.08	12.7	5	57	38	0.1	5.9	64.1	13.4	16.7	0.1	0.8
118	23	0.81	0.06	12.5	4	44	52	0.1	10.2	55.6	15.5	18.8	0.2	0.8
124	24	0.81	0.07	12.3	0	0	0	NA	3.4	72.6	5.4	18.6	0.0	0.3
130	24	0.86	0.06	13.8	6	64	30	0.1	NA	NA	NA	NA	NA	NA
136	22	0.61	0.05	13.1	0	0	0	NA	7.0	77.9	4.2	10.9	0.1	0.4
142	15	0.33	0.02	15.8	0	0	0	NA	NA	NA	NA	NA	NA	NA
148	23	0.52	0.04	13.4	0	0	0	NA	0.6	85.0	3.7	10.8	0.0	0.3
154	22	0.56	0.04	12.9	NA	NA	NA	NA	0.5	81.0	10.6	7.9	0.0	1.3
160	22	0.58	0.06	10.6	NA	NA	NA	NA	NA	NA	NA	NA	NA	NA
166	20	0.53	0.05	10.2	NA	NA	NA	NA	2.5	76.2	11.9	9.4	0.0	1.3
172	22	0.56	0.05	10.4	NA	NA	NA	NA	NA	NA	NA	NA	NA	NA
178	22	0.54	0.04	13.6	0	0	0	NA	NA	NA	NA	NA	NA	NA
184	20	0.56	0.04	13.6	NA	NA	NA	NA	NA	NA	NA	NA	NA	NA
190	23	0.53	0.04	12.9	NA	NA	NA	NA	0.5	77.8	13.5	8.3	0.0	1.6
196	23	0.53	0.04	12.9	NA	NA	NA	NA	6.5	79.7	8.2	5.5	0.1	1.5
202	21	0.6	0.04	13.6	0	0	0	NA	0.8	74.7	7.7	16.8	0.0	0.5
226	22	0.53	0.04	12.6	0	0	0	NA	1.6	75.4	7.1	15.9	0.0	0.4
238	21	0.55	0.04	12.6	NA	NA	NA	NA	NA	NA	NA	NA	NA	NA
244	20	0.57	0.04	12.9	NA	NA	NA	NA	0.9	77.7	12.4	9.0	0.0	1.4
250	22	0.56	0.05	12.3	0	0	0	NA	1.9	73.7	4.8	19.6	0.0	0.2
256	23	0.6	0.06	10.6	NA	NA	NA	NA	4.7	82.7	7.5	5.1	0.1	1.5
262	20	0.52	0.06	9.0	NA	NA	NA	NA	1.3	79.4	11.5	7.8	0.0	1.5

Table 2A (*continued*)

Depth (cm)	$CaCO_3$ (wt%)	OC (wt%)	TN (wt%)	OC/TN	Coarse fraction constituents				Clay minerals					
					B (%)	P (%)	K (%)	B/P	S (%)	I (%)	K (%)	Ch (%)	S/I	K/Ch
268	19	0.55	0.06	9.8	NA	NA	NA	NA	NA	NA	NA	NA	NA	NA
274	19	0.58	0.05	10.9	0	0	0	NA	1.0	75.7	12.1	11.2	0.0	1.1
280	20	0.56	0.05	11.3	NA	NA	NA	NA	NA	NA	NA	NA	NA	NA
286	19	0.72	0.04	16.3	NA	NA	NA	NA	1.1	78.1	14.5	6.3	0.0	2.3
292	20	0.53	0.04	13.2	NA	NA	NA	NA	NA	NA	NA	NA	NA	NA
298	20	0.55	0.05	12.1	NA	NA	NA	NA	6.2	80.9	8.2	4.7	0.1	1.7
300	20	0.57	0.05	12.1	0	0	0	NA	2.9	71.8	8.6	16.6	0.0	0.5
304	20	0.58	0.05	12.4	NA	NA	NA	NA	NA	NA	NA	NA	NA	NA
310	22	0.57	0.05	12.2	NA	NA	NA	NA	1.6	82.8	7.3	8.4	0.0	0.9
316	21	0.55	0.05	11.7	NA	NA	NA	NA	NA	NA	NA	NA	NA	NA
322	21	0.52	0.04	11.7	0	0	0	NA	2.0	69.2	7.2	21.6	0.0	0.3
328	22	0.58	0.04	13.4	NA	NA	NA	NA	NA	NA	NA	NA	NA	NA
334	20	0.56	0.04	12.6	0	0	0	NA	2.3	72.5	13.2	12.0	0.0	1.1
340	20	0.52	0.04	12.5	NA	NA	NA	NA	NA	NA	NA	NA	NA	NA
344	19	0.46	0.03	14.0	NA	NA	NA	NA	1.2	72.1	8.4	18.3	0.0	0.5

Note: 0 indicates values < 0.1. OC: organic carbon; TN: total nitrogen; B: benthic foraminifers; P: planktonic foraminifers; K: keels; S: smectite; K: kaolinite; I: illite; Ch: chlorite; NA: data not available.

of HF, HNO_3, $HClO_4$ and heated in a microwave and digested. The solution was then transferred to a Teflon beaker and evaporated to near dryness on a hot plate. The residue was dissolved in 20 ml of 1:1 HNO_3 and made up to final volume. The aliquots were analysed for Rb, Sr, Sm and Nd concentrations (Table 3; Figs. 6–7) with a Perkin Elmer Elan DRC II ICP-MS at the National Geophysical Research Institute (NGRI), Hyderabad, India. An International standard MAG-1 (Henderson and Pankhurst, 1984; Govindaraju, 1994) was used to check the accuracy. The precision of the measurement based on duplicate analysis is as follows: Rb $\pm$ 0.73 ppm, Sr $\pm$ 1.02 ppm, Sm $\pm$ 0.4 ppm, Nd $\pm$ 0.21 ppm.

The powdered $<2\,\mu m$ fractions of the clay samples were digested with HF–HNO_3 acid mixture. The Sr and REE were then separated using columns packed with cation exchange resin (DOWEX AG-50 WX 8). Nd was separated from the REE fraction with columns packed with HDEHP-coated biobeads anion resin. The Sr and Nd isotope ratio measurements were carried out on a VG 354E thermal ionization mass spectrometer (TIMS) in the dynamic triple collector mode at the NGRI, Hyderabad. The $^{87}Sr/^{86}Sr$ ratios were corrected for fractionation with $^{86}Sr/^{88}Sr = 0.1194$ and normalized to SRM 987 standard value of 0.710220 ± 0.000024 (2 sigma S.D.; $n = 10$). $^{143}Nd/^{144}Nd$ ratios were corrected for fractionation with $^{146}Nd/^{144}Nd = 0.7219$ and normalized to La Jolla standard value of 0.511850 ± 0.000010 (2 sigma S.D.; $n = 8$). For the total process the blank value for Sr was <250 pg and for Nd isotopic measurements it was negligible (<25 pg). The Sr–Nd isotopic compositions are shown in Table 3. The down core distribution and *X*–*Y* plot of the Sr–Nd concentrations and their isotopes, together with available data for the Bengal Fan sediments are shown in Figs. 6 and 7.

The planktonic foraminifer '*Globigerinoides ruber*' was hand picked from the coarse fraction of the sediments of core 1. The age of this foraminifer in four sediment samples (Table 4) was measured by the ^{14}C method using accelerator mass spectrometer (AMS) at the Woods Hole Oceanographic Institution (WHOI), USA. The measured ages were calibrated (Table 4), following

Table 2B
Distribution of $CaCO_3$, coarse fraction constituents and clay minerals in AAS37/2

Depth (cm)	$CaCO_3$ (%)	Coarse fraction constituents				Clay minerals					
		B (%)	P (%)	K (%)	B/P	(S) (%)	(K) (%)	(I) (%)	(Ch) (%)	S/I	K/Ch
0	52	2	7	91	0.26	25.7	8.1	59.4	6.8	0.4	1.2
4	53	3	3	93	0.89	35.3	7.8	50.3	6.5	0.7	1.2
6	NA	1	5	94	0.12	27.3	11.0	54.0	7.7	0.5	1.4
8	51	NA	NA	NA	NA	NA	NA	NA	NA	NA	NA
10	NA	1	11	88	0.06	28.2	8.2	52.3	11.3	0.5	0.7
12	54	NA	NA	NA	NA	NA	NA	NA	NA	NA	NA
14	NA	1	21	78	0.04	22.8	8.3	59.8	9.0	0.4	0.9
16	57	NA	NA	NA	NA	NA	NA	NA	NA	NA	NA
18	NA	2	49	49	0.04	24.1	9.7	58.1	8.1	0.4	1.2
20	61	NA	NA	NA	NA	NA	NA	NA	NA	NA	NA
22	NA	1	48	51	0.02	23.5	9.6	60.8	6.0	0.4	1.6
24	57	NA	NA	NA	NA	NA	NA	NA	NA	NA	NA
26	NA	1	23	76	0.02	19.7	9.6	66.1	4.6	0.3	2.1
28	54	NA	NA	NA	NA	NA	NA	NA	NA	NA	NA
30	NA	1	21	78	0.05	22.6	9.3	60.2	8.0	0.4	1.2
32	34	NA	NA	NA	NA	NA	NA	NA	NA	NA	NA
34	NA	5	16	79	0.29	21.1	9.5	63.0	6.3	0.3	1.5
36	51	NA	NA	NA	NA	NA	NA	NA	NA	NA	NA
38	NA	NA	NA	NA	NA	32.9	8.3	50.5	8.3	0.7	1.0
40	47	NA	NA	NA	NA	NA	NA	NA	NA	NA	NA
42	NA	3	17	80	0.16	33.2	9.1	48.5	9.3	0.7	1.0
44	41	NA	NA	NA	NA	33.17	NA	NA	NA	NA	NA
46	36	2	7	92	0.23	NA	NA	NA	NA	NA	NA
48	38	1	10	89	0.09	12.6	8.2	72.7	6.6	0.2	1.2
50	26	NA	NA	NA	NA	27.1	6.4	58.7	7.9	0.5	0.8
52	18	1	9	91	0.1	16.6	4.9	71.0	7.6	0.2	0.6
54	15	0	3	97	0	10.0	3.3	79.2	7.5	0.1	0.4
58	16	0	0	0	0	11.1	2.3	80.6	6.1	0.1	0.4
62	15	0	0	0	0	11.2	2.3	79.8	6.6	0.1	0.4
66	24	0	0	0	0	9.5	2.4	81.3	6.8	0.1	0.4
70	17	0	0	0	0	8.1	2.1	85.2	4.6	0.1	0.5
72	19	1	15	84	0.05	5.6	3.1	85.7	5.6	0.1	0.6
84	39	0	0	0	0	4.2	4.9	81.0	9.9	0.1	0.5
88	49	0	0	0	0	5.2	1.7	86.4	6.7	0.1	0.3
92	18	5	19	76	0.29	10.1	2.0	79.9	7.9	0.1	0.3
96	25	15	33	51	0.46	8.8	4.3	80.4	6.6	0.1	0.7
100	21	8	25	67	0.3	11.3	3.8	76.6	8.3	0.1	0.5
102	52	NA	NA	NA	NA	NA	NA	NA	NA	NA	NA
104	NA	0	0	0	0	8.4	2.3	83.2	6.0	0.1	0.4
106	53	NA	NA	NA	NA	NA	NA	NA	NA	NA	NA
108	NA	3	13	84	0.22	14.1	2.9	77.5	5.5	0.2	0.5
110	51	0	0	0	0	8.8	4.0	80.8	6.4	0.1	0.6

Note: 0 indicates values <0.1. B: benthic foraminifers; P: planktonic foraminifers; K: keels; S: smectite; K: kaolinite; I: illite; Ch: chlorite; NA: data not available.

Stuiver et al. (1998). Detailed procedure for calibration is given in Rao et al. (2003). The reservoir age (~400 yr) of the ^{14}C of the surface ocean at low-latitudes was subtracted from the raw ^{14}C ages, and corrected ages were used for discussion.

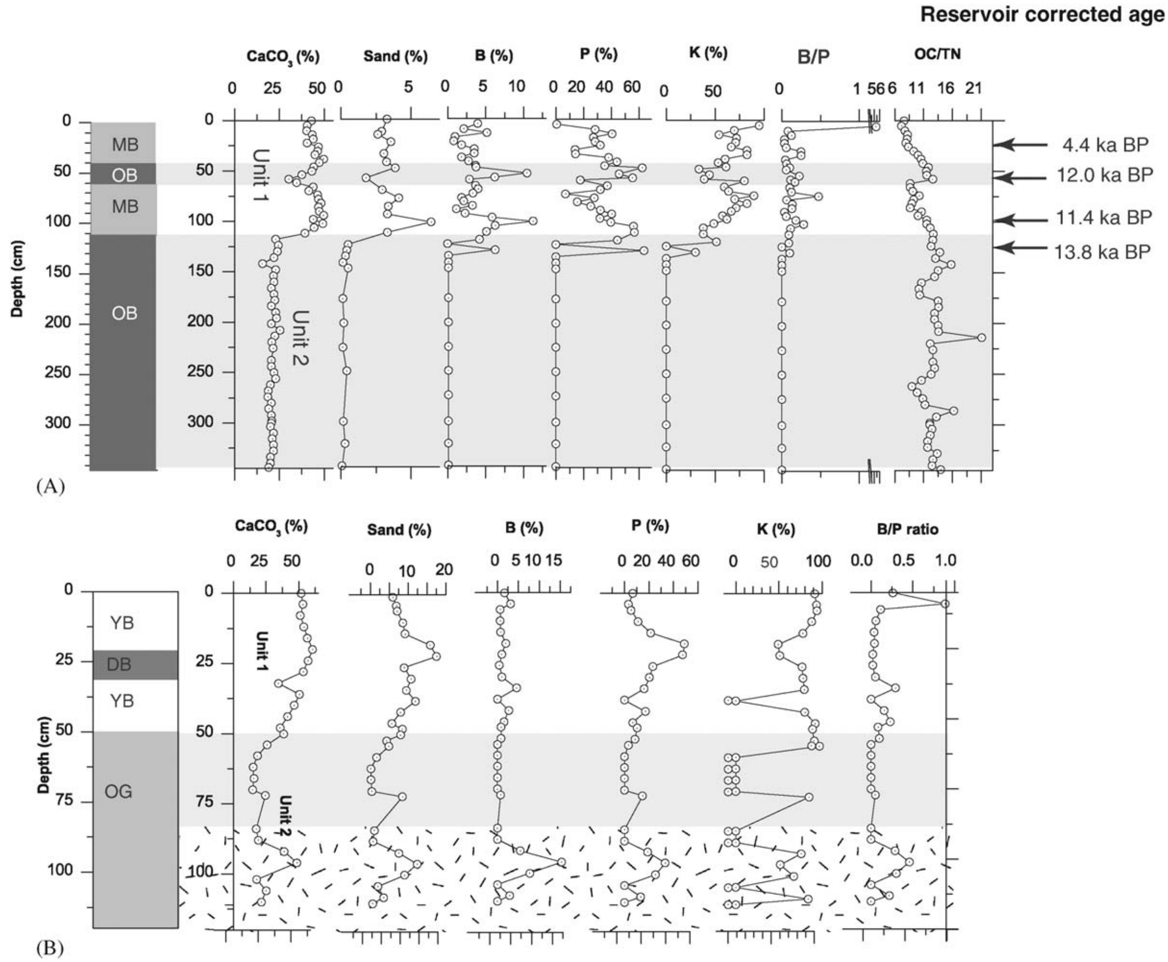

Fig. 2. (A) Downcore variations of the sedimentological parameters (colour, $CaCO_3$ content, sand, benthic (B), planktonic (P) foraminifers and partly dissolved skeletals (keels—K) and organic carbon (OC)/total nitrogen (TN)) in sediment core SK148/2. OB—olive black, MB—moderate brown. (B) Downcore variations of the sedimentological parameters (colour, $CaCO_3$ content, sand, benthic (B), planktonic (P) foraminifers and partly dissolved skeletals (keels—K)) in sediment core AAS37/2. OG—olive grey, YB—yellowish brown, DB—dark brown).

5. Results

The cores exhibit distinct downcore variations in several sedimentological (colour, $CaCO_3$, grain size, mineralogy, magnetic susceptibility, constituents of the coarse fraction) properties, Rb, Sr, Sm, Nd concentrations and Sr–Nd isotopic ratios. On the basis of their distribution, the sediments in each core are divided into two distinct sedimentary units, unit 2 sediments in the lower section and unit 1 sediments in the upper section (Figs. 2A–B). The boundary between unit 1 and unit 2 sediments in each core varies and is placed at ~112 cm in core 1 and ~50 cm in core 2.

5.1. Unit 1 sediments

5.1.1. Colour

Unit 1 sediments in core 1 are 112 cm thick and largely moderate brown in colour. A thin (20 cm) olive black sediment layer occurs at ~50 cm (Fig. 2A). The sediments in core 2 are 50 cm

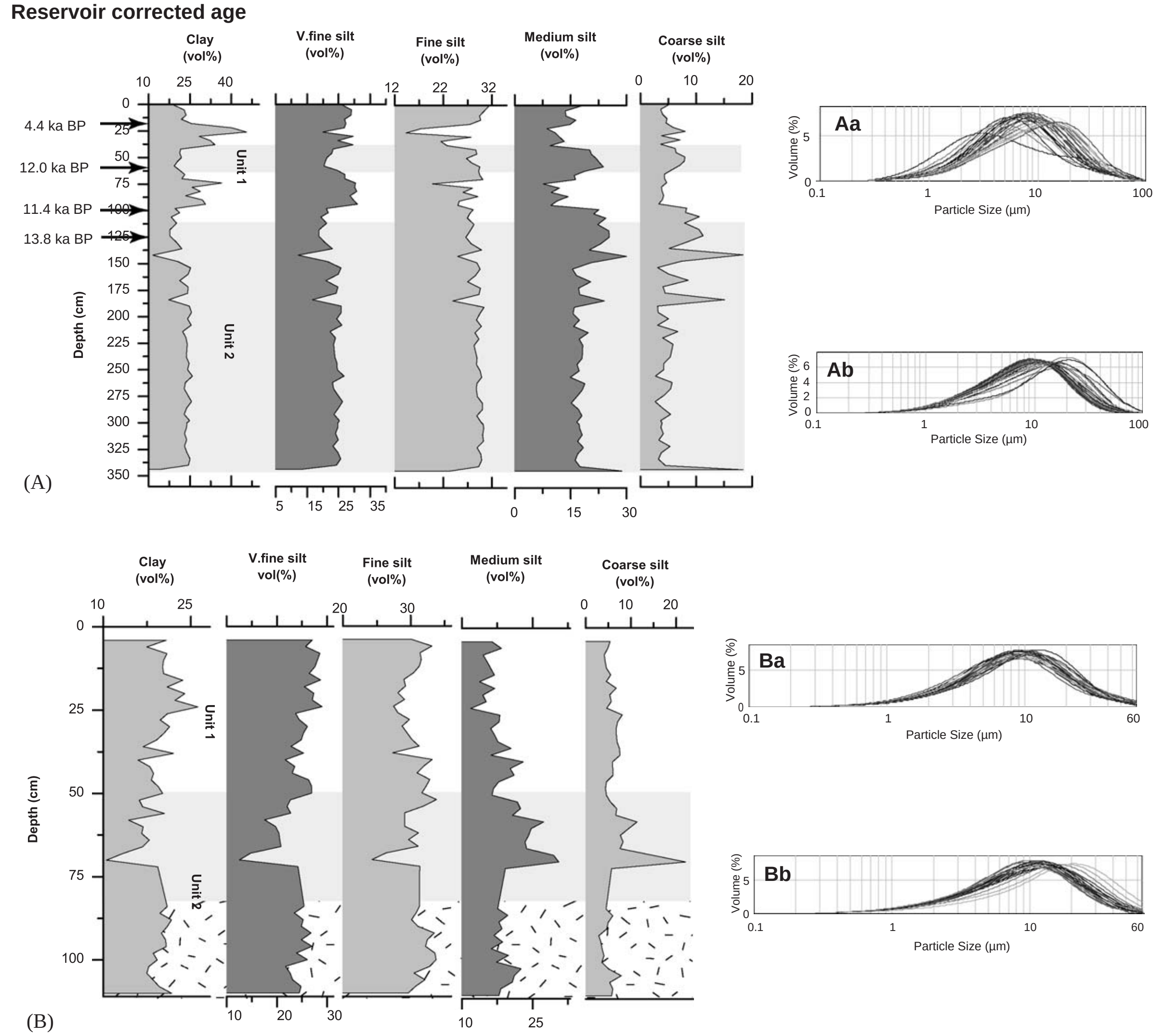

Fig. 3. (A) Grain size variations (following Wentworth's grade scale) in mud fraction (<63 μm size) of the sediment in core SK148/2. (Aa) and (Ab) show the grain size frequency curves in the mud fraction for unit 1 and unit 2, respectively. (B) Grain size variations (following Wentworth's grade scale) in mud fraction (<63 μm size) of the sediment in core AAS37/2. (Ba) and (Bb) show the grain size frequency curves in mud fraction of the sediment in unit 1 and unit 2, respectively.

thick and largely yellowish brown in colour. A dark brown sediment layer occurs at 24–33 cm (Fig. 2B).

5.1.2. $CaCO_3$ and coarse fraction

The $CaCO_3$ content of core 1 is lower (30–50%; Table 2A) than that of core 2 (34–61%; Table 2B). It is low in the olive black sediment layer (Fig. 2A). $CaCO_3$ content increases gradually from the base (30%) to the core top (54%) in core 2, and is found to be higher in yellowish brown sediments (Fig. 2B). Sand content in core 1 (<5%) is lower than in core 2 (up to 17%) and dominated by biogenic constituents. Partly dissolved skeletal constituents (keels) are predominant in the sand fraction. The increase in the proportions of keels

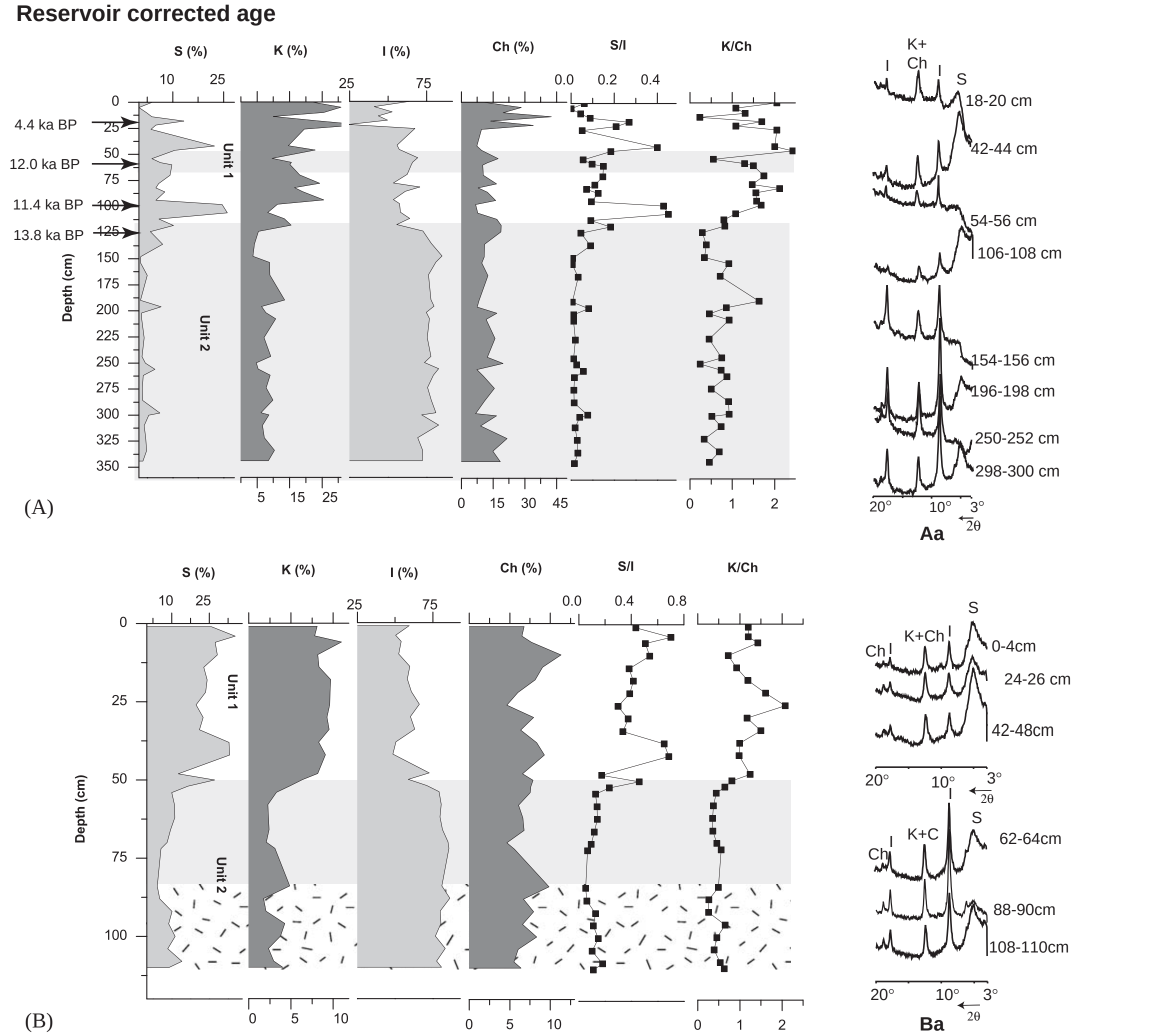

Fig. 4. (A) Downcore distribution of smectite (S), kaolinite (K), illite (I), chlorite (Ch), S/I and K/Ch ratios in core SK148/2. (Aa) Representative X-ray diffractograms of the core at different intervals. (B) Down core distribution of smectite (S), kaolinite (K), illite (I), chlorite (Ch), S/I and K/Ch ratios in core AAS37/2. (Ba) Representative X-ray diffractograms of the core at different intervals.

coincides with the decrease in the percentage of planktic and benthic foraminifers and vice versa (Figs. 2A–B). The benthic (B)/planktic (P) foraminifers ratio is, in general, low (<0.3) in both the cores, except at the core top and base of unit 1 (Fig. 2B). The OC/TN ratios in unit 1 decrease from base to the core top and range between 7.1 and 15.8 with higher ratios in olive black sediment (Fig. 2A). SEM studies of the carbonate free samples indicate that the siliceous fragments constitute $<1\%$ in both the cores.

5.1.3. Grain size

Among different size fractions of the terrigenous mud ($<63\,\mu m$), the volume percent of clay and very fine silt dominate at certain intervals of moderate brown sediments and the volume percent of medium silt and coarse silt dominate the olive black sediment layer (Fig. 3A). The size frequency curves of this unit are unimodal, but variations in median and mean size of the mud resulted in shifting of the curves (see Fig. 3Aa). However, in core 2, the volume percent of clay, very fine silt

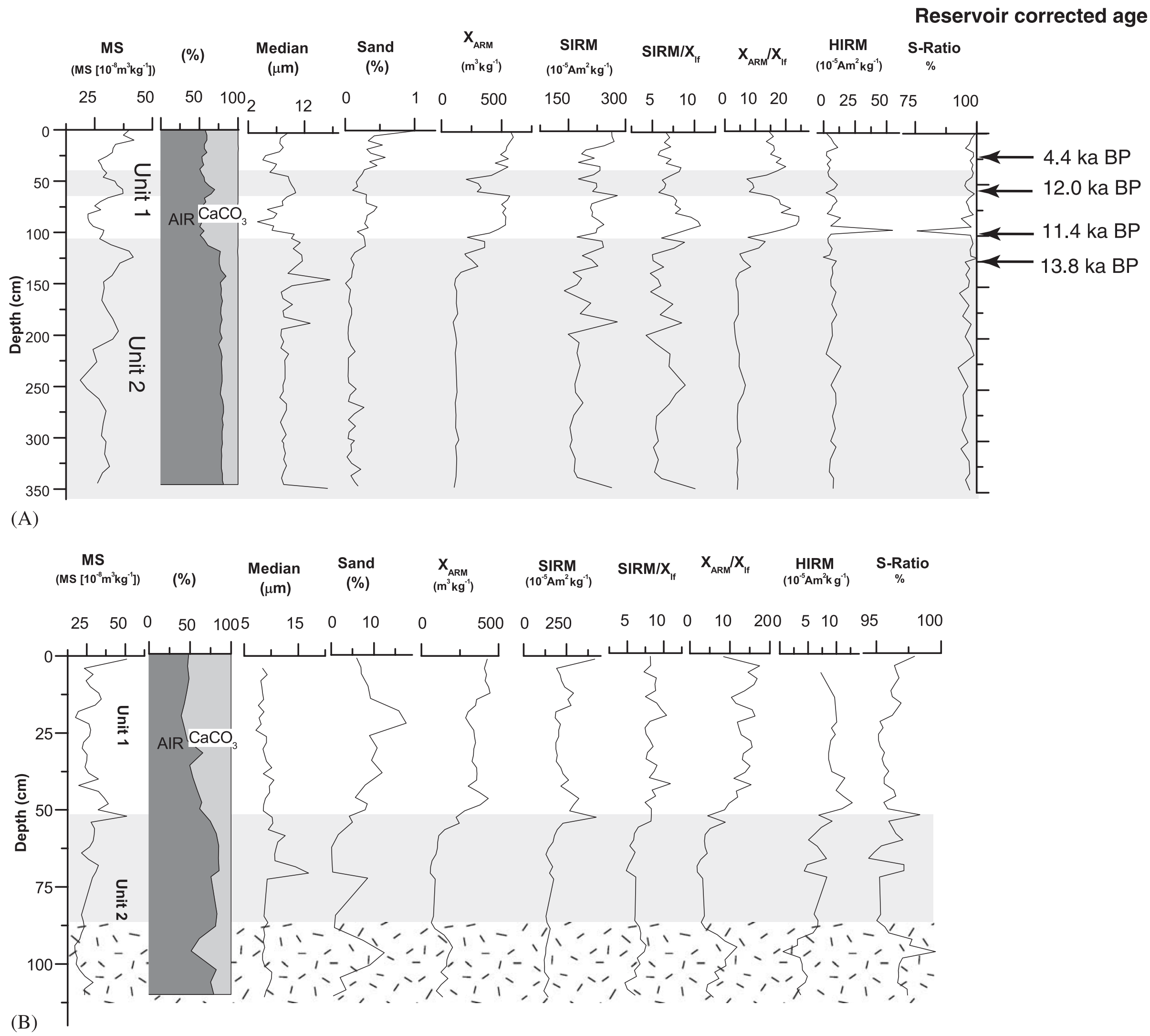

Fig. 5. Downcore variations in rock-magnetic properties of the sediments in core SK148/2 (A), and in AAS37/2 (B).

and fine silt appear to dominate the mud fraction (Fig. 3B). In the size frequency curves the sediments of this unit display unimodal characteristics without much variation in median and mean, leading to the overlapping of the curves (Fig. 3Ba).

5.1.4. Clay minerals

Illite (I), chlorite (Ch), kaolinite (K) and smectite (S) are dominant clay mineral groups present in both the cores (Tables 2A–B). Although illite and chlorite contents are found to be dominant in core 1 (varying from 24% to 70% and 7% to 42%, respectively), smectite (up to 26%) and kaolinite (up to 37%) proportions are higher in this unit (Fig. 4A). High proportions of kaolinite and K/Ch and S/I ratios correspond to moderate brown sediments and low proportions of smectite and kaolinite to olive black sediment layers (Fig. 4Aa). In core 2, illite (48–73%) is the most dominant clay mineral followed by smectite

Table 3
The Rb, Sr, Sm and Nd concentrations in bulk samples and Sr–Nd isotopes of $<2\,\mu m$ fraction of the sediment at different intervals of cores 1 and 2

	Depth (cm)	Rb (ppm)	Sr (ppm)	Sm (ppm)	Nd (ppm)	$^{87}Sr/^{86}Sr$	$^{143}Nd/^{144}Nd$	ε_{Nd}
Core 1 (SK148/2)								
Unit 1	10	NA	NA	NA	NA	0.730072	NA	NA
	14	98.41	99.28	2.72	11.36	NA	0.511709	−18.12
	18	NA	NA	NA	NA	0.726283	NA	NA
	30	110.00	125.92	3.69	16.00	NA	0.511499	−22.2
	54	NA	NA	NA	NA	0.727143	NA	NA
	66	104.89	96.43	2.75	12.63	0.726985	0.511504	−22.12
	106	113.10	117.77	3.41	14.58	NA	0.511614	−19.98
Unit 2	142	172.86	118.88	5.39	27.71	0.734977	0.511798	−16.39
	202	195.74	112.27	5.41	29.20	0.734851	0.511875	−14.88
	274	213.56	111.10	5.39	NA	0.735052	0.511756	−17.21
	300	190.53	119.83	5.43	NA	0.734719	NA	NA
Core 2 (AAS37/2)								
Unit 1	2	129.89	114.52	3.78	16.68	0.722563	0.511827	−15.82
	22	118.94	122.04	3.73	17.43	0.716956	0.511889	−14.61
	34	119.66	130.15	3.75	16.05	0.717330	NA	NA
	50	151.22	100.75	4.00	19.71	0.722452	NA	NA
Unit 2	62	174.86	103.36	4.81	26.11	0.734091	NA	NA
	72	174.91	111.01	5.17	NA	0.733363	0.511928	−13.85
	84	176.81	111.19	5.05	26.14	0.725971	NA	NA
	100	179.26	109.71	4.52	NA	0.726036	0.511958	−13.26

NA: data not available.

(up to 35%), kaolinite (up to 11%) and chlorite (up to 10%). The smectite and kaolinite contents showed significant increase at the expense of illite (Fig. 4Ba). The S/I and K/Ch ratios are high, reaching up to 0.7 and 1.6, respectively (Table 2B).

5.1.5. *Rock magnetic properties*

Magnetic susceptibility (χ_{lf}) values in core 1 range between 22 and 42 SI units and between 18 and 51 SI units in core 2. MS variations are coherent with that of the AIR and inversely proportional to $CaCO_3$ in both the cores (Figs. 5A–B). In core 2, relatively high MS values occur at the core top and base of unit 1. In core 1 median grain size of the mud fraction ($<63\,\mu m$) varies from 5 to $10\,\mu m$, and peaks of relatively high median size correlate well with peaks of high MS (Fig. 5A). χ_{ARM} and χ_{ARM}/χ_{lf} values increase with the decrease of MS, and SIRM and SIRM/χ_{lf} are coherent with that of MS variations. Uniformly low HIRM and high S-ratio% are characteristic of unit 1 (Fig. 5A).

In core 2, MS shows no relationship with median grain size of the mud. χ_{ARM}, χ_{ARM}/χ_{lf} and SIRM/χ_{lf} are higher than those of unit 2 of the same core. SIRM variations are coherent with those of MS values. HIRM values are higher at the base of unit 1 and decrease towards the core top, whereas S-ratio% are high at the base and core top and low in the centre (Fig. 5B).

5.1.6. *Rb, Sr, Sm, Nd concentrations and Sr–Nd isotopes*

Unit 1 sediment of core 1 showed lower Rb, Sr, Sm and Nd concentrations than that of core 2 (Table 3). Lower Rb, Sm and Nd concentrations and $^{87}Sr/^{86}Sr$ ratios and more negative ε_{Nd} values are characteristic of unit 1 sediments, compared to those of unit 2 of the same cores (Table 3; Figs. 6–7). In core 2, the Sr values of unit 1 are higher than those of unit 2.

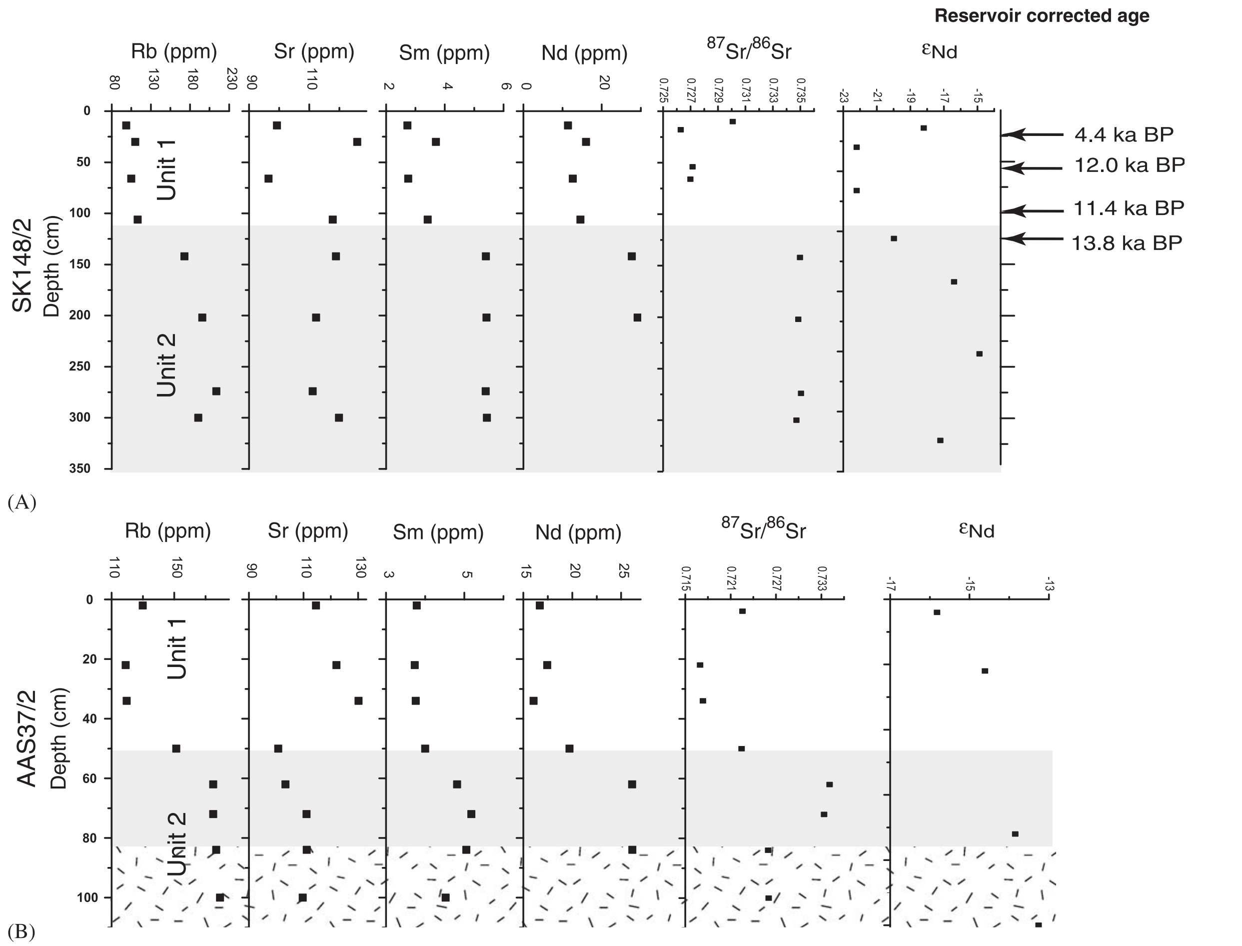

Fig. 6. Downcore variations in Rb, Sr, Sm, Nd concentrations and Sr and Nd isotopes in core SK148/2 (A) and AAS37/2 (B).

5.1.7. Age

The sediment interval at 120–130 cm unit 2 in core 1 (Table 4) yielded a reservoir corrected age of 13,750 ^{14}C yr BP. The age of the sediments close to the base of unit 1 (90–100 cm) is 11,350 ^{14}C yr BP. The olive black intermittent layer at 58–60 cm and sediment interval at 18–24 cm yielded ages 12,000 ^{14}C yr BP and 4420 ^{14}C yr BP (Table 4), respectively.

5.2. Unit 2 sediments

5.2.1. Colour

The unit 2 sediments are olive black/olive grey in colour throughout the section (Figs. 2A–B).

5.2.2. $CaCO_3$ and coarse fraction

The $CaCO_3$ content is low, ~15–25% in core 1 and ~20% in core 2 (Tables 2A–B), except at intervals 80 and 95 cm, where it shoots up to 49% (Fig. 2B). The coarse fraction contains mica flakes and quartz grains. In core 1, keels (K) and planktic (P) and benthic (B) foraminifers are absent (Table 2A; Fig. 2A), whereas in core 2, a relatively high percentage of keels occurs at the boundary of unit 1 and unit 2 and at 85–105 cm (Table 2B; Fig. 2B). The B/P ratio is extremely low, except at the bottom of the core (Fig. 2B). The OC/TN ratios are high ranging between 9 and 21 (Fig. 2A). SEM studies indicate that coccoliths are extremely rare constituents in core 1 and the upper half of

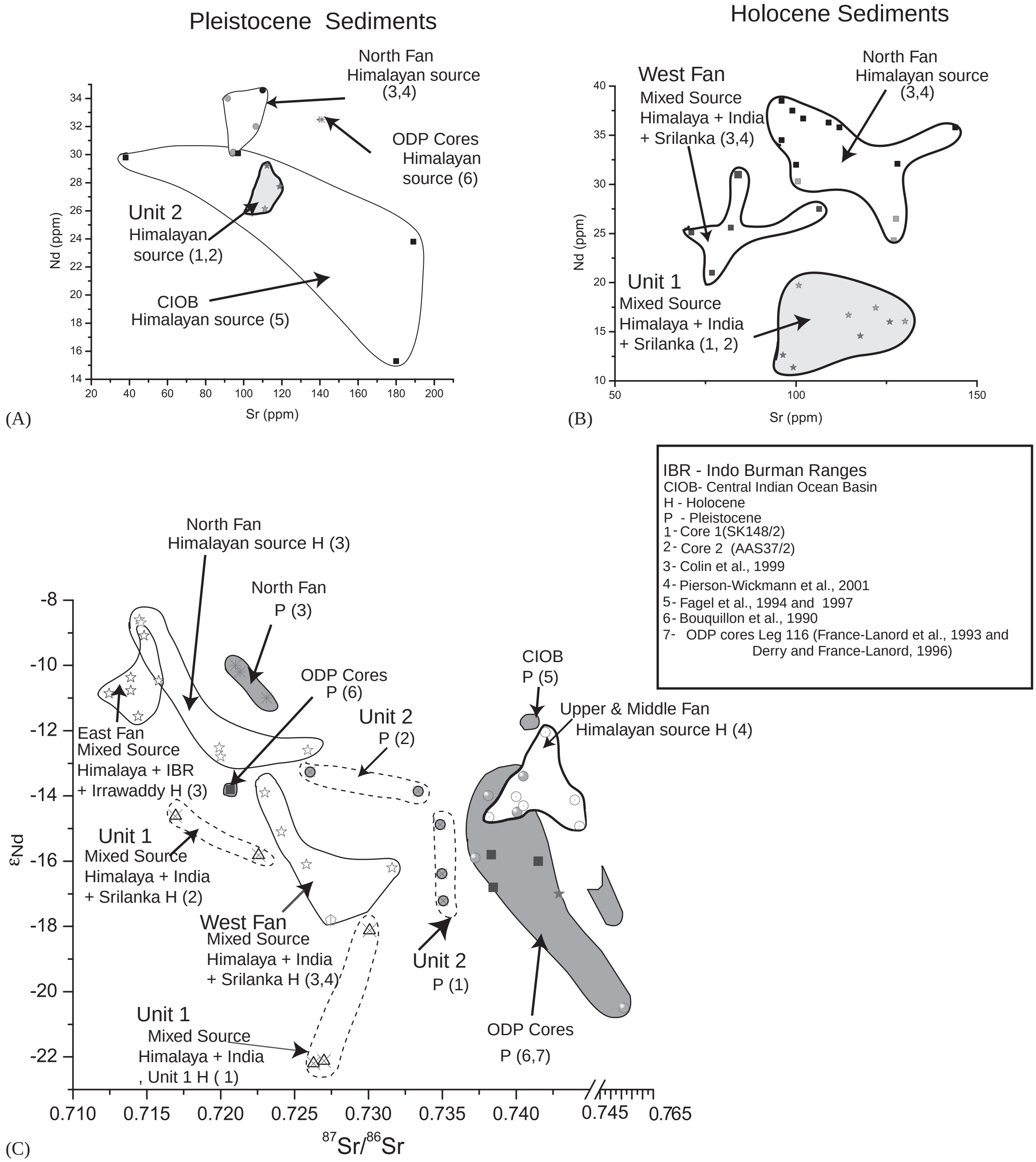

Fig. 7. *X–Y* plot of the Sr and Nd concentrations of sediment samples (core 1 and 2) together with the reported values of Fan sediments during the Pleistocene (A) and Holocene (B). (C) *X–Y* plot of Sr and Nd isotopes of core 1 and 2 (marked with dotted outlines) together with the reported values of the Fan sediments. Holocene sediments are shown in white background and those of Pleistocene age in grey background.

Table 4
AMS ^{14}C ages of the sediments in core 1 (SK148/2)

Sediment intervals in the core (cm)	Reference no. at WHOI	Measured ^{14}C age (yr BP)	Reservoir corrected age (yr BP)	Calibrated age (yr BP)
18–24	44018	4820±30	4420	4924
58–60	44019	12,400±50	12,000	13,605
98–100	44020	11,750±60	11,350	13,089
120–130	44021	14,150±70	13,750	16,271

WHOI: Woods Hole Oceanographic Institution.

unit 2 in core 2, but dominate in the lower half of unit 2 in core 2. Siliceous fragments are rare to absent in unit 2 of both the cores.

5.2.3. Grain size

Silt fractions dominate in sediments of both the cores (Fig. 3A). In core 1, very fine silt, fine silt and medium silt make up the large volume of the terrigenous mud (<63 μm) (Fig. 3A). The size frequency curves show largely unimodal distribution without much variation in median and mean size, leading to the overlapping of many curves (Fig. 3Ab). Even in core 2 the volume percent clay is less (see Fig. 3B) than that of very fine silt, fine silt, medium silt and coarse silt. The grain size frequency curves also showed unimodal distribution (Fig. 3Bb).

5.2.4. Clay minerals

High illite and chlorite, and low S/I (0.01–0.18) and K/Ch (0.24–1.63) ratios are characteristic in both the cores (Tables 2A–B). Smectite and kaolinite contents are extremely low in core 1 (Table 2A; Fig. 4A), whereas in core 2, their proportions increase at the top and base of unit 2 (Table 2B; Fig. 4B).

5.2.5. Rock magnetic properties

In core 1, MS values show marginal variations (19–42 SI units). All other rock magnetic properties (χ_{ARM}, SIRM, χ_{ARM}/χ_{lf}, SIRM/χ_{lf}, HIRM and S-ratios) are consistently uniform and their values are lower than those of unit 1 sediments (see Fig. 5A). In core 2, MS values are also lower than those of unit 1, and higher values occur at the boundary between units 1 and 2. The χ_{ARM} and SIRM values are coherent with MS. Lower SIRM/χ_{lf} and χ_{ARM}/χ_{lf} are characteristic of this unit. Low HIRM and high S-ratio% occur at the base and top of this unit and low S-ratio% in the centre (Fig. 5B).

5.2.6. Rb, Sr, Sm, Nd concentrations and Sr–Nd isotopes

High concentrations of Rb, Sm and Nd, $^{87}Sr/^{86}Sr$ and more radiogenic ε_{Nd} are characteristic of this unit (2), compared to that of unit 1 of the same cores (Table 3; Fig. 6). In core 1, the Sr, Sm and Nd concentrations and their isotopic ratios are consistently uniform (Figs. 6–7). Sr values in unit 2 of both the cores are comparable (Table 3).

6. Discussion

6.1. Importance of rock-magnetic properties

The basic parameters that indicate variations in magnetic mineral concentrations are χ_{lf}, χ_{ARM} and SIRM. χ_{lf} represents total contribution from magnetic minerals and is sensitive to the larger magnetic grain sizes in the range of large pseudo-single domain (PSD) and multidomain (MD) magnetic grain sizes. The χ_{ARM} and SIRM increase in value with an increase in concentration of fine magnetic grain sizes (single domain) (Bloemendal et al., 1992). The interparametric ratios (χ_{ARM}/χ_{lf} and χ_{ARM}/SIRM) vary inversely with magnetic grain size and can be used to assess the relative change in concentrations of finer magnetic grain sizes. SIRM/χ_{lf}, χ_{ARM}/χ_{lf} ratios are low for multidomain (MD > 1 μm) and superparamagnetic (SP < 0.03 μm) grains and high for single domain (0.03–1 μm) grains (Maher and Taylor, 1988). The S-ratio% and HIRM reflect variations in the magnetic mineral assemblage. Values of S ratio% ~100 indicate a high proportion of magnetite, whereas lower values indicate an increasing proportion of hematite and goethite, and the parameters vary with the concentration of high coercivity minerals (Thompson and Oldfield, 1986; Robinson, 1986).

High S-ratio% and low HIRM in both units of core 1 indicate that magnetite is the predominant magnetic mineral. The coincidence of decrease in χ_{lf} and median grain size with the increase in SIRM/χ_{lf}, χ_{ARM}/χ_{lf} ratios at certain intervals in both unit 1 and 2 (Fig. 5A) suggests the presence of finer magnetic grain sizes (single domain), probably due to the formation of authigenic bacterial magnetite. Flat magnetic properties in unit 2 reflect the fact that the sediments are derived largely from a single source. Variations in χ_{lf}, χ_{ARM} and SIRM in unit 1 sediments indicate that these parameters are influenced by grain size. Although the variations in χ_{lf}, χ_{ARM} and SIRM are coherent with each other, HIRM values increase at the transition zone between unit 1 and unit 2 in core 2 (Fig. 5B). This implies increased hematite/goethite content and thus variable source sediments in this core.

6.2. Age of the sediments

The transition between unit 1 and 2 sediments in core 1 occurs at ~112 cm (Fig. 2A). The age, 13,750 ^{14}C yr BP at 120–130 cm (Table 4), implies that the unit 2 sediments are of Late Pleistocene age, which continued to deposit even after the Last Glacial Maximum (LGM ~18,000 ^{14}C yr BP) and in the initial phase of deglaciation and slow rise in sea-level. Fairbanks (1989) reported that the rise of sea-level in the first phase of deglaciation (17,100–12,500 yr BP) was only 20 m.

The age 11,350 ^{14}C yr BP at 90–100 cm (Table 4) suggests that the age at 112 cm (base of unit 1) might at least be 12,000 ^{14}C yr BP, implying that the unit 1 sediments started depositing at ~12 ^{14}C kyr BP. This age corresponds well with the starting of the melt water pulse 1A, during which rapid sea-level rise of 24 m occurred in < 1000 yr (Fairbanks, 1989). This also implies that unit 2 sediments terminated most probably as a result of this sharp rise in sea-level.

The corrected date of 12,000 yr BP at 58–60 cm (Table 4) corresponds to the intermittent olive black sediment layer and is older and stratigraphically inconsistent (Fig. 2A). The age at 18–24 cm in unit 1 is 4420 ^{14}C yr BP, suggesting that the top 20 cm of unit 1 deposited at a rate of ~4 cm/ka. This agrees well with the earlier reported rates of sedimentation (2–4 cm/ka) in this area (Udintsev, 1975; Prell et al., 1980). If one excludes the olive black layer, the remaining 92 cm thick sediments of unit 1 were deposited in 12,000 yr, suggesting that the average rate of sedimentation was ~7 cm/ka.

Absolute ages were not determined for core 2 sediments. Unit 1 sediments of this core are thinner than those in core 1. Because of their location in the Bay, one would expect higher rates of sedimentation at core 1 and lower rates at core 2. Since core 2 showed similar changes in lithofacies as that in core 1, we presume that the unit 2 sediments are of Late Pleistocene age and unit 1 sediments started depositing since 12 ka.

6.3. Unit 2 sediments

The unit 2 sediments are largely olive black/grey in colour, marked by low $CaCO_3$, OC/TN, more quartz and mica in the coarse fraction, and abundant illite in < 2 μm fraction. Very fine silts and fine silts dominate the siliciclastic mud (Figs. 3A–B). Grain size frequency curves (Figs. 3Ab, 3Bb) exhibit unimodal distribution. These characteristics point to abundant terrigenous material, most probably derived from a single source. Flat rock magnetic properties (Fig. 5A) and consistent and uniform Rb, Sr, Sm, Nd concentrations and Sr isotopic ratios (Table 3; Figs. 6, 7A) also suggest a single source.

The mean size of the muds (< 10 μm) in unit 2 sediments is within the size range (6.7–7.8 μm) reported for hemipelagic muds (Joseph et al., 1998). However, the coarse fraction is largely devoid of biogenic components, except at the base of unit 2 in core 2 (Fig. 2B). Only a few coccoliths are seen under SEM. The locations of the cores are also away from the continental margins, implying that the unit 2 sediments are unlikely to be hemipelagic muds.

Distal turbidites are generally centimeter thick beds and show graded bedding of silts and sand. The sediments are strongly skewed towards the coarser end of the silt fractions (medium and coarse silt), and their mean grain size ranges between 9 and 29.6 μm (Joseph et al., 1998). Unit 2 sediments are dominated by fine silt and very fine silt and the median grain size is $<10\,\mu m$. No sedimentary structures were observed during subsampling of the sediment cores onboard. Neither graded bedding nor sharp boundaries of the individual layers were found. The term 'turbidite', therefore, may not strictly apply for these sediments.

The characteristics of unit 2 sediments, however, correspond well with those of 'hemiturbidites' described by Stow and Wetzel (1990) for the distal Bengal Fan sediments. Hemiturbidites are bioturbated (seen only under X-ray images), dark to light gray muds (very fine silts: 7.5–7.9 ∅ with symmetrical to slightly positively skewed distributions) of about 10–100 cm thick with indistinct bed boundaries and few (rare to absent) calcareous microfossils. These are deposited slowly from an essentially stationary dilute suspension cloud that is produced from the dying stages of a large low-concentration turbidity current. We therefore suggest that unit 2 sediments represent hemiturbidites.

The age of the hemiturbidites at 120–130 cm in core 1 is 13,750 ^{14}C yr BP (Table 4). However, the hemiturbidites continued up the core to 113 cm (Fig. 2A). This implies that these muds must have been older than 13 ^{14}C kyr BP. It is likely that these muds started depositing after the fall of sea-level during the last glaciation. The rapid fall of eustatic sea-level, starting at $\sim$24 ^{14}C kyr, resulted in a significant erosion of the continental margin sediments and enhanced turbidity current activity. Enhanced turbidite deposition during low stands of sea-level, sometimes continuing until 12 ^{14}C kyr BP, was reported on the Amazon Fan, the Missisipi Fan and the Bengal Fan (Manley and Flood, 1988; Kolla and Macurda, 1988; Bouma et al., 1989; Kolla and Perlmutter, 1993; Weber et al., 1997). Prins et al. (2000) reported a sedimentary succession that consists of turbidites draped by a very homogenous hemipelagic mud unit, which in turn is overlain by a calcareous ooze unit in the Indus Fan. In other words, turbidity currents were much more active and turbidites reached farther during the low stands of sea-level than during the high stands.

6.3.1. Provenance of unit 2 sediments

The clastic sediments of unit 2 are dominated by quartz and mica in the coarse fraction and by illite and chlorite in the $<2\,\mu m$ fraction (Figs. 4A–B). These sediments may not have originated from the western margin of the Bay of Bengal. Because the hinterland geological formations (charnockite gneisses and schistose rocks and coastal Tertiaries; Fig. 1B) of SE India and Sri Lanka weather under humid tropical conditions, kaolinite, smectite and illite, in order of abundance, are the major clay minerals (see Rao and Kessarkar, 2001). On the other hand, illite and chlorite are largely the products of physical weathering, and clay mineral suites of the Ganges and its tributaries reflect a glacial derivative from the Himalayan Mountain System (Naidu et al., 1985). High illite and chlorite with traces or absence of smectite and kaolinite were reported in suspended and bed load of the Himalayan rivers, its tributaries and estuarine and shelf sediments off Ganges (Subramanian, 1980; Naidu et al., 1985; Rao, 1991). Illite and chlorite-rich clays in Pleistocene turbidites of the Bengal Fan undoubtedly are of Himalayan source (Cochran et al., 1989; Stow et al., 1990; Bouquillon et al., 1990; France-Lanord et al., 1993; Derry and France-Lanord, 1996). The low S/I and K/Ch ratios in unit 2 of these two cores thus suggest that the clastic sediments are derived from the Himalayan rocks and soils in the drainage basin of the Himalayan rivers and transported to the Bay of Bengal by the G–B River system.

The average Sr–Nd concentrations of unit 2 sediments (hemiturbidites) in both the cores are comparable and similar to those of the Himalayan sourced sediments deposited in different regions of the Bengal Fan (see Table 5; Figs. 6–7). On the Sr vs. Nd plot (Fig. 6A) these sediments fall within the area of sediments of Central Indian Basin (Fagel et al., 1994, 1997) and close to that of the Northern Fan (Colin et al., 1999; Pierson-Wickmann et al., 2001), which are of dominant Himalayan origin. Similarly, the $^{87}Sr/^{86}Sr$ ratios of the sediments (0.73472–0.73505 in core 1; 0.72597–0.73409 in core 2; Table 3) and ε_{Nd} of core 1 (−14.88 to −17.21) are within the range of values reported for the particulate flux of the Ganges River (0.72271–0.75238; −14.8 to −17.7; Galy et al., 1999; Dowling et al., 2003). The ε_{Nd} values of core 2 (−13.26 to −13.85) are slightly more radiogenic than that of the Ganges. Moreover, the Sr–Nd isotope values of unit 2 (Table 3) lie between the values of the Pleistocene sediments of the North Fan (0.7210–0.7231, −10 to −11; Colin et al., 1999) and Upper and Middle Fan (0.740–0.750, −15.5 to −14.6; Pierson-Wickmann et al., 2001). The Sr–Nd isotope values of the Pleistocene sediments of the Central Indian Basin (0.7409; −11.75; Fagel et al., 1994) are also different.

Despite the fact that the sediments at all these locations originated from the NBOB (Colin et al., 1999; Pierson-Wickmann et al., 2001; Fagel et al., 1994), varied Sr–Nd isotope ratios occur (Table 5), may be for the following reasons. (a) Although transported by turbidity currents, the hemiturbidites are more fine-grained than turbidite sequences, and obviously some differences in isotope values are expected. (b) It may be due to the analysis of a different fraction of the sediment. For example, we have analysed the carbonate- and organic-matter-free $<2\,\mu m$ fraction of the sediments, whereas others analysed carbonate-free bulk samples (Colin et al., 1999; Pierson-Wickmann et al., 2001; Table 5). (c) It is well known that the Sr isotopes vary with grain size and are very sensitive to the sedimentary cycle. Sr is an ambiguous tracer (Biscaye and Dasch, 1971; Revel et al., 1996). On the other hand, Nd isotopic composition may be due to the mixing of sediments derived from different sources (Grousset et al., 1988; Revel et al., 1996; Innocent et al., 2000; Kessarkar et al., 2003). It is likely that sediment originating from different sources was mixed with sediments of primarily Himalayan origin, which diluted the Sr–Nd signals. On the basis of Sr–Nd signals, Fagel et al. (1994) suggested that the sediments of the Central Indian Basin were dominantly from the Himalayan flux with some contribution from the Chaggos–Laccadive Ridge. Similarly, Colin et al. (1999) reported that the sediments of the eastern Bengal Fan and western Bengal Fan were dominantly of Himalayan source with some contribution from the Irrawady River and Godavari–Krishna, respectively. On the $^{87}Sr/^{86}Sr$ vs. ε_{Nd} plot (Fig. 7C) unit 2 sediments fall between the West Fan sediments and Pleistocene sediments (of the ODP cores) of the distal Bengal Fan, derived from the turbidity currents originating at the NBOB. We therefore suggest that the source for clastic sediments of unit 2 (in core 1 and upper half of unit 2 in core 2) may be the Himalayas, transported to the NBOB by the G–B River system and then to the distal Fan by turbidity currents. The Afanasiy–Nikitin Seamount is located close to core 2 (see Fig. 1A), and weathered basalts and carbonates were recovered at summit levels (Banakar et al., 1997). Smectite-enriched intervals (Fig. 4Ba), low Sr isotopic ratios (Fig. 5B), more radiogenic Nd isotopes and biogenic constituents at the lower half of unit 2 sediments in core 2 (Fig. 2B) suggest that the locally derived sediment from the seamount may have been transported to the core site and diluted the predominant Himalayan flux (Table 3).

6.4. Unit 1 sediments

Unit 1 sediments are largely light coloured and show higher OC/TN, $CaCO_3$, planktic foraminifers, keels, smectite and kaolinite contents, lower $^{87}Sr/^{86}Sr$ and more negative ε_{Nd} than those of unit 2 of the same core. Average median grain size of the sediment is also much lower. MS values, though varied, show strong coherence with AIR.

The higher proportions of keels followed by planktic and a few benthic foraminifers (Figs. 2A–B) indicate that unit 1 sediments are pelagic. The increased percentage of keels at certain intervals may be because of the (a) influence of the lysocline or carbonate compensation depth (CCD), (b) intrusion and corrosive

Table 5
Average Rb, Sr, Sm, Nd concentrations and Sr and Nd isotopic data from the Bengal Fan

Sample locations	Age	Sample type	Rb (ppm)	Sr (ppm)	Sm (ppm)	Nd (ppm)	$^{87}Sr/^{86}Sr$	$\varepsilon_{Nd(0)}$	Inferences of the source	Ref
Lower Fan (SK148/2)	H	Bulk°	106.00	85.0	3.2	13.7	0.72762# (0.72628–0.73007)	−20.60# (−22.2 to −18.12)	Mixed source Himalaya + Indian Peninsula	1
	P	Bulk°	192.5	115.5	5.4	28.5	0.73489# (0.73472–0.73505)	−16.16# (−17.21 to −14.88)	Himalaya	
Distal Fan (AAS37/2)	H	Bulk°	129.9	116.9	3.8	17.5	0.71982# (0.71696–0.72256)	−15.21# (−15.82 to −14.61)	Mixed source Himalaya + Indian Peninsula + Sri Lanka	2
	P	Bulk°	176.5	108.5	4.9	26.1	0.72986# (0.72597–0.73409)	−13.55# (−13.85 to −13.26)	Mixed Source Himalaya + Afanasiy–Nikitin Seamount	
Northern Bay of Bengal	H	Bulk°	NA	118.3	NA	27.0	0.72191 (0.71990–0.72587)	−12.63 (−12.8 to −12.5)	Himalaya	3
	P	Bulk°	NA	94.4	NA	32.0	0.72183 (0.72101–0.72315)	−10.63 (−11 to −10.2)	Himalaya	
Eastern Bay of Bengal	H	Bulk°	NA	149.0	NA	23.3	0.71444 (0.71232–0.71719)	−10.16 (−11.5 to −8.6)	Mixed source Himalaya + Indo-Burman Ranges + Irrawaddy source	
	P	Bulk°	NA	108.0	NA	24.6	0.71728 (0.71332–0.72230)	−9.38 (−11.5 to −7.0)	Mixed source Himalaya + Indo-Burman Ranges + Irrawaddy source	
Western Bay of Bengal	H	Bulk°	NA	84.0	NA	24.8	0.72612 (0.72305–0.73156)	−15.32 (−16.2 to −13.9)	Mixed source Himalaya and Indian Peninsula	
Upper and Middle Fan	H	Bulk°	NA	93.5	NA	30.4	0.729625 (0.72936–0.72989)	−10.55 (−11.7 to −9.4)	Mixed source Indo-Burman Ranges + Himalaya	4
	P	Bulk°	NA	99.0	NA	31.2	0.72459 (0.72400–0.72527)	−10.86 (−11.1 to −10.6)	Mixed source Indo-Burman Ranges + Himalaya	
Upper and Middle Fan	H	Bulk°	NA	109.0	NA	35.1	0.74241 (0.73811–0.74723)	−14.20 (−15.3 to −12.0)	Himalaya	
	P	Bulk°	NA	110.0	NA	34.6	0.74159 (0.74507–0.73811)	−15.05 (−15.50 to −14.6)	Himalaya	
Lower Fan	H	Bulk°	NA	84.0	NA	31.0	0.72748	−17.8	Mixed source Himalaya and Sri Lanka	
Distal Bengal Fan	P	Clays	128.0	141.0	6.4	32.5	0.73844	−16.8	Himalaya	5
Central Indian Basin	P	Clays	105.0	109.0	4.2	22.5	0.7409	−11.75	Himalaya	6

H—Holocene; P—Pleistocene; °—Carbonate-free samples; #—Carbonate-free clays; NA—data not available; 1—Core 1, this study; 2—Core 2, this study; 3—Colin et al. (1999); 4—Pierson-Wickmann et al. (2001); 5—Bouquillon et al. (1990); 6—Fagel et al. (1994, 1997).

effect of the Antarctic Bottom Water (AABW) and (c) early diagenesis. The water depths at core 1 (3600 m) and core 2 (4000 m) are close to the lysocline (~3700–3900 m) and well above the CCD (~4500–4800 m; see Kolla et al., 1976). The CCD has not changed much in this area for the last 2–3 Myr (Stow et al., 1990). The AABW occurs below 2000 m and has been traced only up to 5°S (Warren, 1982). The cores (core 1 at 10°N and core 2 at 2°S latitude; Table 1) are located far north of the AABW. The intervals of low organic carbon coincide with a high percentage of keels and vice versa (Fig. 2A). These suggest that the high percentage of keels may be due partly to the influence of the lysocline and early diagenesis. Segall and Kuehl (1992) and Weber et al. (2003) reported that the western side of the active channel received only pelagic sediments during the Holocene.

Hemiturbidites were produced from the dying turbidity current activity and stationary mud suspensions at the distal fan (Stow and Wetzel, 1990). The change in lithofacies from hemiturbidites (unit 2) to calcareous-dominated pelagic sediments (unit 1) at ~12 kyr BP implies that the large-scale turbidity current transport was switched off after 12 kyr BP, perhaps by the rapid rise in sea-level associated with melt water pulse 1A (Fairbanks, 1989). The continued sea-level rise during the Holocene may have resulted in the confinement of turbidity–current activity to upper fan regions and prevalence of pelagic sedimentation at the core sites. Stow et al. (1989) reported a drape of pelagic calcareous ooze of Holocene age in the distal Bengal Fan sediments.

6.4.1. *Provenance of unit 1 sediments*

Increased proportions of smectite and kaolinite and high S/I and K/Ch ratios (Figs. 4A–B) reflect increased chemical weathering products, which are well reported in the sediments of the east coast of India. Although illite is a weathering product of the gneissic and schistose rocks of the Eastern Ghats and Sri Lankan province, its proportions are found to be lower than those of kaolinite (Rao, 1991). Moreover, the sediments off the Krishna and Godavari contain abundant smectite and minor kaolinite and chlorite. Higher illite followed by smectite and kaolinite in unit 1 sediments of these cores most probably indicates that the clay mineral suites derived from the hinterland formations of SE India and Sri Lanka and transported by a southerly current (prominent both during SW and NE monsoon in this region; Shetye et al., 1993) may have admixed with the clays brought to the NBOB by the G–B River system and transported to the core site by the southward-drifting plume (Shetye et al., 1991). This results in mixed mineral suites at the core sites. Colin et al. (1999) reported that the sediments of the West Fan are an admixture of sediments from the G–B River system and western margins of the Bay of Bengal.

Except Sr in core 2, the concentrations of Rb, Sr, Sm and Nd in unit 1 sediments are lower than those of unit 2 (Table 3). The Sr–Nd concentrations of unit 1 sediments are close to those of the Holocene sediments of the Western Fan and Lower Bengal Fan sediments (Table 5). The Rb and Sm concentrations resemble those in the south Indian formations (Peucat et al., 1989). On the Sr vs. Nd plot (Fig. 6B) unit 1 sediments fall below the mixed source and Himalayan source sediments, suggesting that they are of mixed sources from the Himalayas and India and Sri Lanka. Reduced $^{87}Sr/^{86}Sr$ ratios and more negative ε_{Nd} values are characteristic of unit 1 (Table 3). The Sr–Nd isotopic ratios are influenced by several factors: (a) higher $^{87}Sr/^{86}Sr$ and more negative ε_{Nd} values are expected from chemical weathering of the older geological formations. For example, the $^{87}Sr/^{86}Sr$ and ε_{Nd} of the tonalitic, granitic and charnockite gneisses of the Archean rocks of southern India range from 0.70232 to 0.72549 and −23 to −44.9, respectively (Peucat et al., 1989). Similarly, varied $^{87}Sr/^{86}Sr$ ratios and ε_{Nd} values were reported for the Highland (0.71886–1.2387; −12 to −30.3), Vijayan (0.70587–0.92174; −4.2 to −10.1) and Wanni (0.71330–0.97792; −4.7 to −19.8) complexes of the Sri Lankan formations (Milisenda et al., 1994). Revel et al. (1996), however, pointed out that the Sr–Nd isotopes of a particular rock sample or geological unit are less representative of the potential source area than estuarine samples or adjacent marine sediments. This is very much evident when one compares the $^{87}Sr/^{86}Sr$ ratios and ε_{Nd} values of unit 1 sediments of core 1 and 2 (Table 3) with those of the kaolinite-rich, smectite and illite sediments (range from 0.7175 to 0.7229 and −18.45 to −20.29, respectively) derived from gneissic and schistose rocks and deposited on the SW continental margin of India (Kessarkar et al., 2003). These indicate that unit 1 sediments are influenced by the older crust material, which has undergone chemical weathering. (b) The $^{87}Sr/^{86}Sr$ ratios usually increase with the increase of clay content (Walter et al., 2000). Despite high proportions of clay and fine silt in unit 1, $^{87}Sr/^{86}Sr$ ratios are lower than those of unit 2. This probably implies mixed sources of sediments in unit 1 sediments. On the $^{87}Sr/^{86}Sr$ vs. ε_{Nd} plot (Fig. 7C) the unit 1 sediments fall away from North Fan and East Fan but are close to those of West Fan, indicating a mixed source with sediment proportions from the G–B River system and SE India and Sri Lanka.

The age of the olive black/dark brown sediment layer in unit 1 is stratigraphically inconsistent (Fig. 2A; Table 4). Although this sediment resembles the unit 2 sediments of the same cores, it has high planktonic foraminifers and high organic carbon in core 1 (Fig. 2A) and high carbonate, sand and planktonic foraminifers in core 2 (Fig. 2B). It is likely that this layer of sediment was reworked and deposited at the core site from the adjacent floor during slack periods of sea-level rise.

Acknowledgements

We thank the Directors of the National Institute of Oceanography, Goa, National Geophysical Research Institute, Hyderabad, and Indian Institute of Geo-magnetism, Alibag, for the facilities and encouragement. We appreciate and thank Dr. S.W.A. Naqvi and Dr. M. Dileep Kumar for providing funds for AMS dating of 4 samples. PMK thanks the Council of Scientific and Industrial Research (CSIR), New Delhi, for the award of Senior Research Fellowship. We thank Dr. V. Ramaswamy for his help with the laser particle size analyser and Mr. Girish Prabhu for XRD work. We thank Drs. V. Balaram and T.G. Rao of NGRI for their help with ICP-MS analysis. This is NIO Contribution no. 3955.

References

Anonymous, 1965. Gazetteer of India Publications Division, Ministry of Information and Broadcasting. Government of India, 1652pp.

Banakar, V.K., Pattan, J.N., Mudholkar, A.V., 1997. Palaeoceanographic conditions during the formation of a ferromanganese crust from the Afanasiy–Nikitin Seamount, North Central Indian Ocean: geochemical evidence. Marine Geology 136, 299–315.

Ben Othman, D., White, W.M., Patchett, J., 1989. The isotopic and trace element composition of sediments: constraints on the genesis of Island arc volcanics and crust-mantle recycling. Earth and Planetary Science Letters 94, 1–21.

Biscaye, P.E., 1965. Mineralogy and sedimentation of deep see clay in the Atlantic Ocean and adjacent sea and oceans. Bulletin of Geological Society of America 76, 803–832.

Biscaye, P.E., Dasch, E.J., 1971. The rubidium and strontium isotope system in deep-sea sediments: Argentine Basin. Journal of Geophysical Research 76, 5087–5096.

Bloemendal, J., King, J.W., Hall, F.R., Doh, S.J., 1992. Rock magnetism of the Late Neogene and Pleistocene deep-sea sediments: relationship to sediment source, diagenetic processes, and sediment lithology. Journal of Geophysical Research 97, 4361–4375.

Bouma, A.H., Coleman, J.M., Stelting, C.E., Kohl, B., 1989. Influence of relative sea level changes on the construction of the Mississipi Fan. Geo-Marine Letters 9, 161–170.

Bouquillon, A., France-Lanord, C., Michard, A., Tiercelin, J.J., 1990. Sedimentology and isotope chemistry of the Bengal Fan sediments: the denudation of the Himalaya. In: Cochran, J.R., Curray, J.R., Sager, W.W., Stow, D.A.V. (Eds.), Proceedings of the Ocean Drilling Program Scientific Results, vol. 116, pp. 43–58.

Brass, G.W., Raman, C.V., 1990. Clay mineralogy of sediments from the Bengal Fan. Proceedings of the Ocean Drilling Program Scientific Results, vol. 116, pp. 35–41.

Chauhan, O.S., Suneethi, J., 2001. 18 Ka BP records of climatic changes, Bay of Bengal: isotopic and sedimentological evidences. Current Science 81, 1231–1234.

Cochran, J.R., 1990. Himalayan uplift, sea level and the record of Bengal Fan sedimentation at the ODP Leg 116 site. In: Cochran, J.R., Curray, J.R., Sager, W.W., Stow, D.A.V. (Eds.), Proceedings of the Ocean Drilling Program Scientific Results, vol. 116, pp. 397–414.

Cochran, J.R., Stow, D.A.V., et al., 1989. Proceedings Ocean Drilling Program Initial Reports, vol. 116. Ocean Drilling Program, College Station, TX, pp. 388.

Colin, C., Turpin, L., Bertauz, J., Desprairies, A., Kissel, C., 1999. Erosional history of the Himalayas and Burman ranges during the last two glacial–interglacial cycles. Earth and Planetary Science Letters 171, 647–660.

Curray, J.R., 1994. Sediment volume and mass beneath the Bay of Bengal. Earth and Planetary Science Letters 125, 371–383.

Curray, J.R., Moore, D.G., 1971. Growth of the Bengal Deep Sea Fan and denudation in the Himalayas. Geological Society of America Bulletin 82, 563–572.

Curray, J.R., Emmel, F.J., Moore, D.G., Raitt, R.W., 1982. Structure, tectonics and geological history of the Northeastern Indian Ocean. In: Nairn, A.E.M., Stechli, F.G. (Eds.), The Ocean Basins and Margins, The Indian Ocean, vol. 6. Plenum Press, New York, USA, pp. 399–450.

Curray, J.R., Emmel, F.J., Moore, D.G., 2003. The Bengal Fan: morphology, geometry, stratigraphy, history and processes. Marine and Petroleum Geology 19, 1191–1223.

Derry, L.A., France-Lanord, C., 1996. Neogene Himalayan weathering history and river $^{87}Sr/^{86}Sr$ impact on the marine Sr record. Earth and Planetary Science Letters 142, 59–74.

Dowling, C.B., Poreda, R.J., Basu, A.R., 2003. The groundwater geochemistry of the Bengal Basin: weathering, chemsorption and trace metal flux to the oceans. Geochimica et Cosmochimica Acta 67, 2117–2136.

Eigenheer, A., Quadfasel, D., 2000. Seasonal variability of the Bay of Bengal circulation inferred from TOPEX/POSEIDON altimetry. Journal of Geophysical Research 105, 3243–3252.

Emmel, F.J., Curray, J.R., 1984. The Bengal Submarine Fan, Northeastern Indian Ocean. Geo-Marine Letters 3, 119–124.

Emmel, F.J., Curray, J.R., 1985. Bengal Fan, Indian Ocean. In: Bouma, H., Normark, W.R., Barner, N.E. (Eds.), Submarine Fans and Related Turbidite Systems. Springer, New York, pp. 107–112.

Fagel, N., Debrabant, P., Andre, L., 1994. Clay supplies in the Central Indian Basin since the Late Miocene, climatic or tectonic control. Marine Geology 122, 151–172.

Fagel, N., Andre, L., Debrabant, P., 1997. Multiple seawater derived geochemical signatures in Indian Ocean pelagic clays. Geochimica et Cosmochimica Acta 61, 989–1008.

Fairbanks, R., 1989. A 17,000 year glacio-eustatic sea level record: influence of glacial melting rates on the Younger Dryas event and deep-ocean circulation. Nature 342, 637–642.

Folk, R.L., 1968. Petrology of the sedimentary rocks. Hemphills, Drawer's M., University Station, Austin, Texas 170pp.

France-Lanord, C., Derry, L.A., Michard, A., 1993. Evolution of the Himalaya since Miocene time: isotopic and sedimentological evidence from the Bengal Fan. In: Treloar, P.J., Searle, M. (Eds.), Journal of Geological Society of London Special Publication, Himalayan Tectonics 74, 603–621.

Galy, A., France-Lanord, C., 2001. Higher erosion rates in the Himalayan geochemical constraints on riverine fluxes. Geology 29, 23–26.

Galy, A., France-Lanord, C., Derry, L.A., 1999. The strontium isotopic budget of Himalayan rivers in Nepal and Bangladesh. Geochimica et Cosmochimica Acta 63, 1905–1925.

Goldberg, E.D., Griffin, J.J., 1970. The sediments of the northern Indian Ocean. Deep-Sea Research Part I 17, 513–537.

Goodbread Jr., S.L., Kuehl, S.A., 1999. Holocene and modern sediment budgets for the Ganges–Brahmaputra river system: evidence for highstand dispersal to flood-plain, shelf and deep-sea depocenters. Geology 27, 559–562.

Govindaraju, K., 1994. Compilation of working values and sample description for 383 geostandards. Geostandards Newsletter 18, 1–158.

Grousset, F.E., Biscaye, P.E., Zindler, A., Prospero, J., Chester, R., 1988. Neodymium isotopes as tracers in marine sediments and aerosols: North Atlantic. Earth and Planetary Science Letters 87, 367–378.

Henderson, P., Pankhurst, R.J., 1984. In: Henderson, P. (Ed.), Rare Earth Element Geochemistry. Elsevier, Amsterdam, pp. 467–495.

Hohndorf, A., Kudrass, R., France-Lanord, C., 2003. Transfer of the Sr isotopic signature of the Himalayas to the Bay of Bengal. Deep-Sea Research Part II 50 (5), 951–960.

Hulsemann, J., 1966. On the routine analysis of carbonates in unconsolidated sediments. Journal of Sedimentary Petrology 36, 622–625.

Innocent, C., Fagel, N., Hillaire-Marcel, C., 2000. Sr–Nd isotope systematics in deep sea sediments: clays-size versus coarse fraction. Marine Geology 168, 79–87.

Joseph, L., Rea, D.K., van der Pluijm, B.A., 1998. Use of grain size and magnetic fabric analyses to distinguish among depositional environments. Paleoceanography 13, 491–501.

Kessarkar, P.M., Rao, V.P., Ahmad, S.M., Babu, G.A., 2003. Clay minerals and Sr–Nd isotopes of the sediments along the western margin of India and their implication for sediment provenance. Marine Geology 202, 55–69.

Kolla, V., Macurda Jr., D.B., 1988. Sea-level changes and timing of turbidity-current events in deep-sea fan systems. In: Wilgus, C.K., Hastings, B.K., Posamentier, H., Van Wagoner, J., Ross, C.A., Kendall, C.G.St.C. (Eds.), Sea-Level Changes: An Integrated Approach. Society of Economic Palaeontologists and Mineralogists, Special Publication No. 42, pp. 381–392.

Kolla, V., Perlmutter, M.A., 1993. Timing of turbidite sedimentation on the Mississippi Fan. American Association Petroleum Geologists Bulletin 77, 1129–1141.

Kolla, V., Rao, N.M., 1990. Sedimentary sources in the surface and near-surface sediments of the Bay of Bengal. Geo-Marine Letters 10, 129–136.

Kolla, V., Be, A.W.H., Biscaye, P.E., 1976. Calcium carbonate distribution in the surface sediments of the Indian Ocean. Journal of Geophysical Research 81, 2605–2616.

Krishnan, M.S., 1968. Geology of India and Burma. Higginbothoms Ltd., Madras 536 pp.

Krishnaswamy, S., Trivedi, J.R., Sarin, M.M., Ramesh, R., Sharma, K.K., 1992. Strontium isotopes and rubidium in the Ganga–Brahmaputra River system: weathering in the Himalaya, fluxes to the Bay of Bengal and contribution to the evolution of oceanic $^{87}Sr/^{86}Sr$. Earth and Planetary Science Letters 109, 243–253.

Kuehl, S.A., Hariu, T.M., Moore, W.S., 1989. Shelf sedimentation off the Ganges–Brahmaputra River system: evidence for sediment bypassing to the Bengal Fan. Geology 17, 1132–1135.

Lightfoot, P.C., Hawkesworth, C.J., Devey, C.W., Rogers, N.W., van Calsteren, P.W.C., 1990. Source and differentiation of Deccan Trap lavas: implications of geochemical and mineral chemical variations. Journal of Petrology 31, 1165–1200.

Maher, B.A., Taylor, R.M., 1988. Formation of ultrafine-grained magnetite in soils. Nature 366, 368–370.

Manley, P.L., Flood, R.D., 1988. Cyclic sediment deposition within Amazon deep-sea fan. American Association Petroleum Geologist Bulletin 72, 912–925.

McCreary, J.P., Han, W., Shankar, D., Shetye, S.R., 1996. Dynamics of the East Indian Coastal Current 2. Numerical solutions. Journal of Geophysical Research 101 (C6), 13,993–14,010.

McLennan, S.M., Tylor, S.R., McCulloch, M.T., Maynard, J.B., 1990. Geochemical and Nd–Sr isotopic composition of deep-sea turbidites: crustal evolution and plate tectonic associations. Geochimica et Cosmochimica Acta 54, 2015–2050.

Milisenda, C.C., Liew, T.C., Hofmann, A.W., Kohler, H., 1994. Nd isotopic mapping of the Sri Lanka basement: update and additional constraints from Sr isotopes. Precambrian Research 66, 95–110.

Milliman, J.D., Syvitski, J.P.M., 1992. Geomorphic/tectonic control of sediment discharge to the ocean: the importance of small mountain rivers. Journal of Geology 100, 525–544.

Naidu, A.S., Mowatt, T.C., Somayajulu, B.L.K., Sreeramachandra, Rao, K., 1985. Characteristics of clay minerals in the bed loads of major rivers of India. In: Degens, E.T., Kempe, S., Herrear, R. (Eds.), Transport of Carbon and Minerals in Major World Rivers, part 3, Mitteilungen aus dem Geologischem paleontogischen Institut., University of Hamburg, SCOPE/UNEP Sounderband Heft 58(5), pp. 559–568.

Peucat, J.J., Vidal, P., Bernard-Griffiths, J., Condie, K.C., 1989. Sr, Nd, and Pb isotopic systematics in the Archean low to high-grade transition zone of southern India: syn-accretion vs. post-accretion granulites. Journal of Geology 97, 537–550.

Pierson-Wickmann, A.-C., Reisberg, L., France-Lanord, C., Kudrass, H.R., 2001. Os–Sr–Nd results from sediments in the Bay of Bengal: implications for sediment transport and the marine Os record. Paleoceanography 16, 435–444.

Prell, W.L., Hutson, W.H., Williams, D.F., Be, A.W.H., Geitzenauer, K., Molfino, B., 1980. Surface circulation of the Indian Ocean during the last glacial maximum, approximately 18000 YBP. Quaternary Research 14, 309–336.

Prins, M.A., Postma, G., Cleveringa, J., Cramp, A., Kenyon, N.H., 2000. Controls on terrigenous sediment supply to the Arabian Sea during the Late Quaternary: the Indus Fan. Marine Geology 169, 327–349.

Ramaswamy, V., Vijay Kumar, B., Parthiban, G., Ittekkot, V., Nair, R.R., 1997. Lithogenic fluxes in the Bay of Bengal measured by sediment traps. Deep-Sea Research Part I 44, 793–810.

Rao, V.P., 1991. Clay mineral distribution in the continental shelf sediments from Krishna to Ganges River mouth, east coast of India. Indian Journal of Marine Sciences 20, 7–12.

Rao, V.P., Kessarkar, P.M., 2001. Geomorphology and geology of the Bay of Bengal and the Andaman Sea. In: Sen Gupta, R., Desa, E. (Eds.), The Indian Ocean: A Perspective, vol. 2. Oxford & IBH, New Delhi, India, pp. 817–868.

Rao, V.P., Rajagopalan, G., Vora, K.H., Almeida, F., 2003. Late Quaternary sea level and environmental changes from relic carbonate deposits of the western margin of India. Proceedings of the Indian Academy of Sciences (Earth and Planetary Sciences) 112, 1–25.

Rea, D.K., 1992. Delivery of Himalayan sediment to the Northern Indian Ocean and its relation to global climate, sea level, uplift and seawater strontium. In: Duncan, R.A., et .al. (Eds.), Synthesis of Results From Scientific Drilling in the Indian Ocean: Geophysical Monograph, vol. 70. pp. 387–402.

Revel, M., Cremer, M., Grousset, F.E., Labeyrie, L., 1996. Grain-size and Sr–Nd isotopes as tracers of paleo-bottom current strength, Northeast Atlantic Ocean. Marine Geology 131, 233–249.

Robinson, S.G., 1986. The Late Pleistocene paleoclimatic record of North Atlantic deep-sea sediments revealed by mineral magnetic measurements. Physics of the Earth and Planetary Interiors 42, 22–47.

Sarin, M.M., Krishnaswamy, S., Dilli, K., Somayajulu, B.L.K., Moore, W.S., 1989. Major ion chemistry of the Ganga–Brahmaputra River system: weathering processes and fluxes to the Bay of Bengal. Geochimica et Cosmochimica Acta 53, 997–1009.

Schott, F.A., McCreary, J.P., 2001. The monsoon circulation of the Indian Ocean. Progress in Oceanography 51, 1–123.

Segall, M.P., Kuehl, S.A., 1992. Sedimentary processes on the Bengal continental shelf as revealed by clay-size mineralogy. Continental Shelf Research 12, 517–541.

Shetye, S.R., Shenoi, S.S.C., Gouveia, A.D., Michael, G.S., Sundar, D., Nampoothiri, G., 1991. Wind-driven coastal upwelling along the western boundary of the Bay of Bengal during the southwest monsoon. Continental Shelf Research 11, 1379–1408.

Shetye, S.R., Gouveia, A.D., Shenoi, S.S.C., Sundar, D., Michael, G.S., Nampoothiri, G., 1993. The western boundary current of the seasonal subtropical gyre in the Bay of Bengal. Journal of Geophysical Research 98 (C1), 945–954.

Shetye, S.R., Gouveia, A.D., Shenoi, S.S.C., Vinayachandran, P.N., Sundar, D., Michael, G.S., Nampoothiri, G., 1996. Hydrography and circulation in the western Bay of Bengal during the northeast monsoon. Journal of Geophysical Research 101, 14011–14025.

Siddiquie, H.N., 1967. Recent sediments of the Bay of Bengal. Marine Geology 5, 249–291.

Stow, D.A.V., Cochran, J.R., ODP 116 Shipboard scientific party, 1989. The Bengal Fan: some preliminary results from ODP drilling. Geo-Marine Letters 9, 1–10.

Stow, D.A.V., Wetzel, A., 1990. Hemiturbidites: a new type of deep-water sediment. In: Cochran, J.R., Curray, J.R., Sager, W.W., Stow, D.A.V. (Eds.), Proceedings of the Ocean Drilling Program Scientific Results, vol. 116, pp. 25–34.

Stow, D.A.V., Amano, K., Balson, P.S., Brass, G.W., Corrigan, J., Raman, C.V., Tiercelin, J.J., Townsend, M., Wijayananda, N.P., 1990. Sediment Facies and processes on the distal Bengal Fan, Leg 116. In: Cochran, J.R., Curray, J.R., Sager, W.W., Stow, D.A.V. (Eds.), Proceedings of the Ocean Drilling Program Scientific Results, vol. 116, pp. 377–396.

Stuiver, M., Reimer, P.J., Bard, E., Beck, J.W., Burr, G.S., Hughen, K.A., Kromer, B., McCormac, F.G., vander Plicht, J., Spurkm, M., 1998. INTCAL 98 radiocarbon age calibration, 24000-0 cal BP. Radiocarbon 40, 1041–1083.

Subramanian, V., 1980. Mineralogical input of suspended matter by Indian Rivers into the adjacent areas of the Indian Ocean. Marine Geology 36, M29–M34.

Suresh, N., Bagati, T.N., 1998. Calcium carbonate distribution in the Late Quaternary sediments of Bay of Bengal. Current Science 74, 977–984.

Thompson, R., Oldfield, F., 1986. Environmental Magnetism. Allen & Unwin Publishers Ltd., UK 227pp.

Udintsev, G.B., 1975. Geological Geophysical Atlas of the Indian Ocean, IOC, UNESCO. Pergamon Press, New York 151pp.

Venkataratnam, K., Biscaye, P.E., 1973. Clay mineralogy and sedimentation in the eastern Indian Ocean. Deep-Sea Research 20, 727–738.

von der Borch, C.C., Sclater, J.C., Stefan Jr., G., Hekinion, R., Johnson, S.A., Mc. Gownan, N., Pimm, A.C., Thompson, R.W., Veevers, J.J., 1972. Deep Sea Drilling Project, Leg 22. Geotimes 17, 15–17.

Walter, H.J., Hegner, E., Diekmann, B., Kuhn, G., Rutgers van der loeff, M.M., 2000. Provenance and transport of terrigenous sediment in the south Atlantic Ocean and their relations to glacial and interglacial cycles: Nd and Sr isotopic evidence. Geochimica et Cosmochimica Acta 64, 3813–3827.

Warren, B.A., 1982. The deep water of the Central Indian Basin. Journal of Marine Research 40 (Suppl.), 823–860.

Weber, M.E., Wiedick, M.H., Kudrass, H.R., Hubscher, C., Erlenkeuser, H., 1997. Active growth of the Bengal Fan during sea level rise and highstand. Geology 25, 315–318.

Weber, M.E., Wiedicke-Hombach, M., Kudrass, H.R., Erlenkeuser, H., 2003. Bengal Fan sediment transport activity and response to climate forcing inferred from sediment physical properties. Sedimentary Geology 155, 361–381.

Wetzel, A., 1990. Consolidation characteristics and permeability of Bengal Fan sediments drilled during Leg 116. In: Cochran, J.R., Curray, J.R., Sager, W.W., Stow, D.A.V. (Eds.), Proceedings of the Ocean Drilling Program Scientific Results, vol. 116, pp. 363–368.